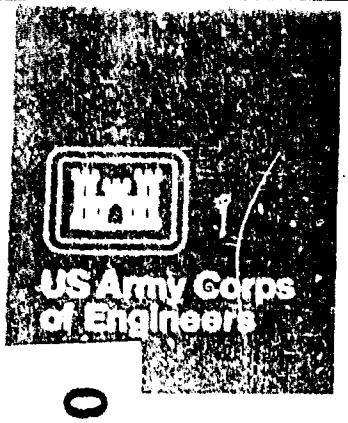

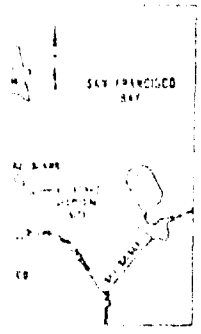

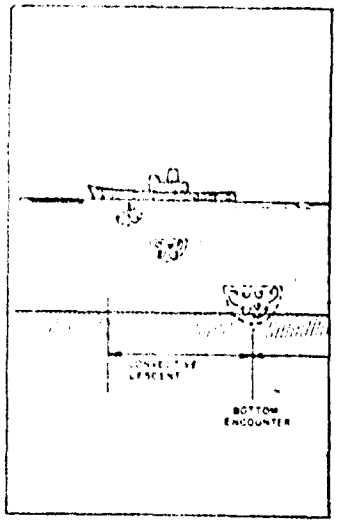

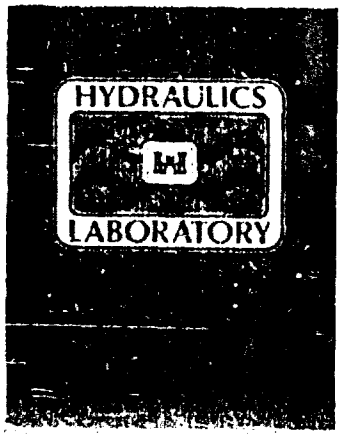

(2)

MISCELLANEOUS PAPER HL-86-1

ALCATRAZ DISPOSAL SITE INVESTIGATION

by

Michael J. Trawle, Billy H. Johnson

Hydraulics Laboratory

DEPARTMENT OF THE ARMY
Waterways Experiment Station, Corps of Engineers
PO Box 631, Vicksburg, Mississippi 39180-0631

March 1986
Final Report

Approved For Public Release; Distribution Unlimited

Prepared for

US Army Engineer District, San Francisco
San Francisco, California 94105

Destroy this report when no longer needed. Do not return it to the originator.

The findings in this report are not to be construed as an official Department of the Army position unless so designated by other authorized documents.

The contents of this report are not to be used for advertising, publication, or promotional purposes. Citation of trade names does not constitute an official endorsement or approval of the use of such commercial products.

Unclassified

SECURITY CLASSIFICATION OF THIS PAGE *(When Data Entered)*

REPORT DOCUMENTATION PAGE

READ INSTRUCTIONS BEFORE COMPLETING FORM

1. REPORT NUMBER: Miscellaneous Paper HL-86-1	2. GOVT ACCESSION NO.
3. RECIPIENT'S CATALOG NUMBER	
4. TITLE *(and Subtitle)*: ALCATRAZ DISPOSAL SITE INVESTIGATION	5. TYPE OF REPORT & PERIOD COVERED: Final report
	6. PERFORMING ORG. REPORT NUMBER
7. AUTHOR(s): Michael J. Trawle Billy H. Johnson	8. CONTRACT OR GRANT NUMBER(s)
9. PERFORMING ORGANIZATION NAME AND ADDRESS: US Army Engineer Waterways Experiment Station Hydraulics Laboratory PO Box 631, Vicksburg, Mississippi 39180-0631	10. PROGRAM ELEMENT, PROJECT, TASK AREA & WORK UNIT NUMBERS
11. CONTROLLING OFFICE NAME AND ADDRESS: US Army Engineer District, San Francisco 211 Main Street San Francisco, California 94105	12. REPORT DATE: March 1986 13. NUMBER OF PAGES: 58
14. MONITORING AGENCY NAME & ADDRESS *(If different from Controlling Office)*	15. SECURITY CLASS. *(of this report)*: Unclassified 15a. DECLASSIFICATION/DOWNGRADING SCHEDULE

16. DISTRIBUTION STATEMENT *(of this Report)*

Approved for public release; distribution unlimited.

17. DISTRIBUTION STATEMENT *(of the abstract entered in Block 20, if different from Report)*

18. SUPPLEMENTARY NOTES

Available from National Technical Information Service, 5285 Port Royal Road, Springfield, Virginia 22161.

19. KEY WORDS *(Continue on reverse side if necessary and identify by block number)*

Alcatraz disposal site (WES)
Dredging—California—San Francisco Bay (LC)
Dredged material (WES)
Waste disposal sites—California—San Francisco Bay (LC)

20. ABSTRACT *(Continue on reverse side if necessary and identify by block number)*

Dredged material from San Francisco Bay has been dumped at the Alcatraz Island open-water disposal site for many years. Since the disposal site lies in an extremely high energy area, historically it has been assumed that the vast majority of the disposed material moves with the current past the Golden Gate Bridge and is then carried out into the ocean. However, recent surveys of the disposal site have shown that a large mound of material, which creates navigation problems, has formed. Since a new dredging project in the area is

(Continued)

DD FORM 1 JAN 73 1473 EDITION OF 1 NOV 65 IS OBSOLETE

Unclassified

SECURITY CLASSIFICATION OF THIS PAGE *(When Data Entered)*

20. ABSTRACT (Continued).

expected to create approximately 5 million cu yd of new material to be disposed at the site over the next 2 years, a major concern is how much of the new material will remain within the disposal site and contribute to the existing mound.

To address ~~the~~ disposal at Alcatraz Island problem, a numerical model has been applied that computes the behavior of a dredged material dump through three phases; namely, convective descent, during which the dump cloud falls under the influence of gravity; bottom collapse, occurring when the descending cloud impacts the bottom; and passive transport-diffusion, commencing when the material transport and spreading are determined more by ambient currents and turbulence than by the dynamics of the disposal operation. The model accounts for land boundaries, depth variations, ambient current variations in three dimensions and in time, several sediment classes within the dredged material, and variations of ambient density profiles in time. A major limitation of the model is that erosion and subsequent redeposition of material deposited on the bottom are not modeled. Therefore results from the numerical model were only used to provide the initial amount and distribution of material deposited within the disposal site. Analytic techniques were subsequently employed to analyze the erosional characteristics of the bottom deposits within the site.

Results of the study show that the dumping of consolidated clumps of clays and silts will contribute to further mounding or accumulation of material within the disposal site since sufficient energy to erode these types of materials at the rate required to avoid mounding does not exist at the site.

(Keywords: (see other side)

PREFACE

The estimation of shcrt-term fate for the open-water disposal of dredged material at the Alcatraz disposal site, documented in this report, was performed for the US Army Engineer District, San Francisco.

The study was conducted in the Hydraulics Laboratory of the US Army Engineer Waterways Experiment Station (WES) during the period April 1984 to August 1984 under the direction of Messrs. H. B. Simmons and F. A. Herrmann, Jr., former and present Chiefs of the Hydraulics Laboratory; Mr. R. A. Sager, Chief of the Estuaries Division; and Mr. M. B. Boyd, Chief of the Hydraulic Analysis Division.

The work was performed and the report prepared by Mr. M. J. Trawle and Dr. B. H. Johnson. Mr. Dave Stewart was the technician for this study. This report was edited by Mrs. Beth F. Vavra, Publications and Graphic Arts Division.

Director of WES was COL Allen F. Grum, USA. Technical Director was Dr. Robert W. Whalin.

CONTENTS

	Page
PREFACE	1
CONVERSION FACTORS, NON-SI TO SI (METRIC) UNITS OF MEASUREMENT	3
PART I: INTRODUCTION	5
Background	5
Objective	5
Approach	6
PART II: DESCRIPTION OF THE NUMERICAL MODEL, DIFID	7
Model Origin	7
Model Approach	7
Theoretical Basis	8
Model Capabilities	14
Assembly of Input Data	16
PART III: TRANSPORT AND RESUSPENSION ANALYSIS	19
Sand Transport and Resuspension	19
Silt and Clay Erosion	21
PART IV: TEST PROGRAM AND RESULTS	22
Test Conditions	22
Discussion of Results	24
PART V: CONCLUSIONS	29
REFERENCES	30
APPENDIX A: DIFID INPUT AND OUTPUT	A1
Input	A1
Output	A1
TABLES A1 and A2	
FIGURES A1-A9	
APPENDIX B: ACKERS-WHITE SAND TRANSPORT CALCULATIONS	B1
TABLES B1-B6	
FIGURE B1	
APPENDIX C: MODIFIED PARTHENAIDES CLAY-SILT RESUSPENSION CALCULATIONS	C1
TABLES C1-C6	
FIGURE C1	

CONVERSION FACTORS, NON-SI TO SI (METRIC)
UNITS OF MEASUREMENT

Non-SI units of measurement used in this report can be converted to SI (metric) units as follows:

Multiply	By	To Obtain
cubic feet	0.02831685	cubic metres
cubic yards	0.7645549	cubic metres
feet	0.3048	metres
pounds (mass)	0.4535924	kilograms
square feet	0.09290304	square metres

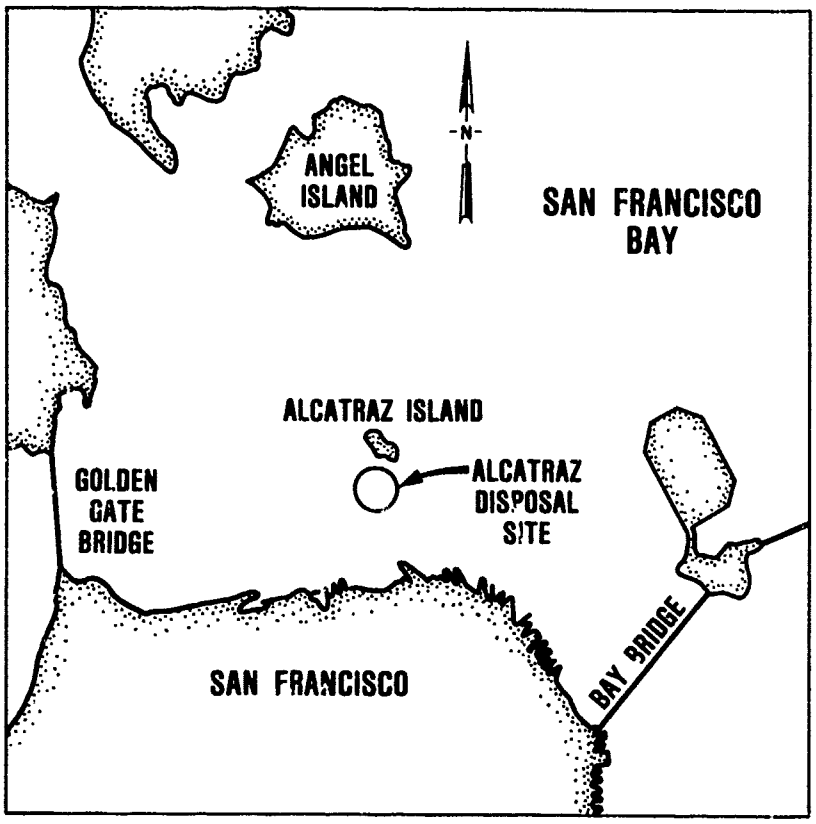

Figure 1. Location of Alcatraz disposal site

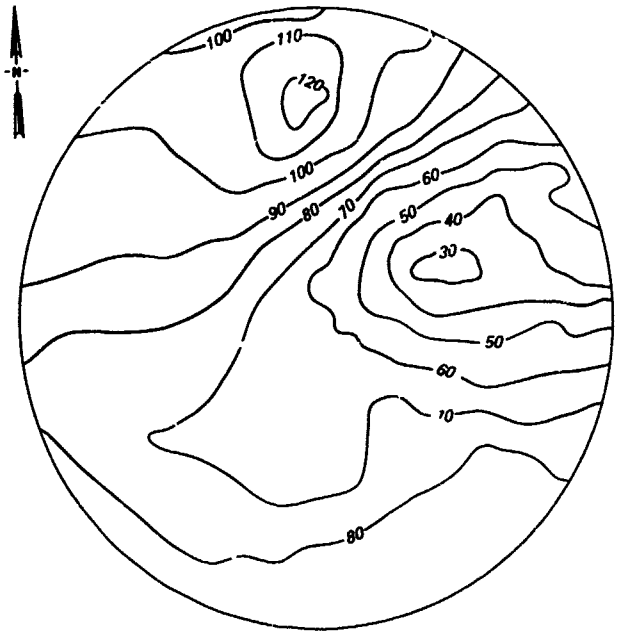

Figure 2. Alcatraz disposal site depth contours from 11 January 1984 survey (soundings in ft mllw)

ALCATRAZ DISPOSAL SITE INVESTIGATION

PART I: INTRODUCTION

Background

1. The Alcatraz disposal site in San Francisco Bay is a dispersive site that is not intended to accumulate disposed material (Figure 1). The strong tidal currents at the site are expected to transport most of the disposed material from the bay through the Golden Gate and out to sea. The disposal site has been in use for about 50 years. For the last 10 years it has been the only authorized open-water disposal site within central San Francisco Bay. Historically, depths within the site have ranged from about 70 to greater than 120 ft.*

2. A recent hydrographic survey has revealed loss of depth at the site and raised questions as to the site's ability to disperse future new work and maintenance material dredged from bay navigation projects. The survey showed that a mound of material existed within the eastern half of the disposal site, resulting in a loss of depth to as little as 28 ft as shown in Figure 2. The loss of depth is a problem for two reasons. First, the site is located in the established shipping lane, thus requiring a depth of 40 ft. Second, since this is the only authorized central bay disposal site, abandonment of this site could mean that dredged material disposal would become much more expensive if an alternate site were selected and approved that was farther from dredging sites.

Objective

3. The objective of the investigation described in this report was to quantitatively estimate the capability of the Alcatraz disposal site to disperse dredged material barge-dumped at the mound location. Specifically, the objective was to estimate both the percentage of dumped material initially

---

* A table of factors for converting non-SI units of measurement to SI (metric) units is presented on page 3.

deposited at the dump site and the percentage of deposited material subsequently resuspended and transported from the dump site under varying hydrodynamic conditions. The investigation did not include the long-term fate of dumped material that leaves the disposal site.

Approach

4. The approach was to first simulate the barge dumping of dredged material using the computer dump model DIFID (Disposal From Instantaneous Dump). This model predicted the portion of the dumped material that was transported from the disposal site by ambient currents before striking the bay bottom and the portion that was deposited within the disposal site. However, a basic limitation of the model was that it did not compute the resuspension and transport of the deposited material. To estimate the amount and rate at which the deposited material was resuspended and transported from the disposal site, an analytic approach was used. The analytic procedure included the use of the Ackers-White transport function for sand transport and the modified Parthenaides equation for the erosion and transport of clays and silts.

5. The computer model, DIFID (Johnson, in preparation), was used to simulate the convective descent, dynamic collapse, and initial deposition phases of barge-dumped material.

6. The Ackers-White (1973) transport formula was used to estimate the capability of the ambient currents to remove the sand initially deposited by DIFID at the dump site.

7. The Parthenaides (1962) erosional equation was used to estimate the resuspension of clays and silts initially deposited by DIFID at the dump site. Appropriate values, based on type of material being dumped, for the critical shear stress for erosion and the erosion rate constant were used in the Parthenaides equation.

8. The Parthenaides equation was also used to estimate erosion of consolidated clay-silt clumps or clods of the type of material to be dumped at the disposal site, again using appropriate values for the critical erosional shear stress and erosion rate constant.

PART II: DESCRIPTION OF THE NUMERICAL MODEL, DIFID

Model Origin

9. The instantaneous dump model (DIFID) was developed by Brandsma and Divoky (1976) for the US Army Engineer Waterways Experiment Station (WES) under the Dredged Material Research Program. Much of the basis for the model was provided by earlier model development by Koh and Chang (1973) for the barged disposal of wastes in the ocean. That work was conducted under funding by the Environmental Protection Agency in Corvallis, Oregon. Modifications to the original model have been made by the Hydraulics Laboratory at WES.

Model Approach

10. The model simulates movement of the disposed material as it falls through the water column, spreads over the bottom, and finally is transported and diffused as suspended sediment by the ambient current. DIFID is designed to simulate the movement of material from an instantaneous dump which falls as a hemispherical cloud. Thus the total time required for the material to leave the disposal vessel should not be substantially greater than the time required for the material to reach the bottom.

11. The model requires that the dredged material be broken into various solid fractions with a settling velocity specified for each fraction. In many cases, a significant portion of the material falls as "clumps" which may have a settling velocity of perhaps 1.0 to 5.0 fps. This is especially true if the dredging is done by clamshell and can be true in the case of hydraulically dredged material if consolidation takes place in the hopper during transit to the disposal site. The specification of a "clump" fraction is rather subjective; therefore the inability to accurately characterize the disposed material in some disposal operations prevents a quantitative interpretation of model results in those operations.

12. As noted, a settling velocity must be prescribed for each solid fraction. A basic assumption is that unless the fraction is specified as being cohesive, in which case the settling velocity is computed as a function of concentration, the settling is considered to occur at a constant rate. In other words, hindered settling is not taken into consideration.

13. Although a variable water depth is allowed over the long-term grid, the collapse of the dredged material cloud on the bottom is somewhat restricted. The effect of a bottom slope is allowed through the incorporation of a gravitational force in the computation of the collapsing cloud. However, a basic limitation still exists in that the bottom is assumed to slope in only one direction over the collapsed region, e.g. bottom collapse on a "mound" where the collapsing cloud runs down the sides is not treated.

14. A major limitation of the model is the basic assumption that once solid particles are deposited on the bottom they remain there. Therefore the models should only be applied over time frames in which erosion of the newly deposited material is insignificant.

15. The model allows for two separate treatments of the passive transport and diffusion phase. In one method, material from the convective descent and dynamic collapse phases is inserted into the fixed long-term grid. Therefore computations at each point of the grid must be made at each time-step in order to march the solution from one time-step to the next. Solid bodies in the field and boundary effects are treated. However, disadvantages are that the vertical distribution is assumed to be that of a "top hat" profile, grid dispersion errors may occur, and the computations can become costly for large grids if many time-steps are computed. A "top hat" profile is represented by a step function that does not allow for any gradual change over the water column. The second approach is to allow material from the descent and collapse phases to be stored in small Gaussian clouds. These clouds are then diffused and transported at the end of each time-step. Computations on the long-term grid are only made at those times when output is desired. However, a limitation when using this approach is that horizontal solid boundaries are not allowed in the long-term grid. This limitation could be removed by employing reflection principles as is currently done at the surface and the bottom.

Theoretical Basis

16. The behavior of the disposed material is assumed to be separated into three phases: convective descent, during which the dump cloud or discharge jet falls under the influence of gravity; dynamic collapse, occurring when the descending cloud either impacts the bottom or arrives at the level of neutral buoyancy at which descent is retarded and horizontal spreading domi-

nates; and long-term passive dispersion, commencing when the material transport and spreading are determined more by ambient currents and turbulence than by the dynamics of the disposal operation. Figure 3 illustrates these phases.

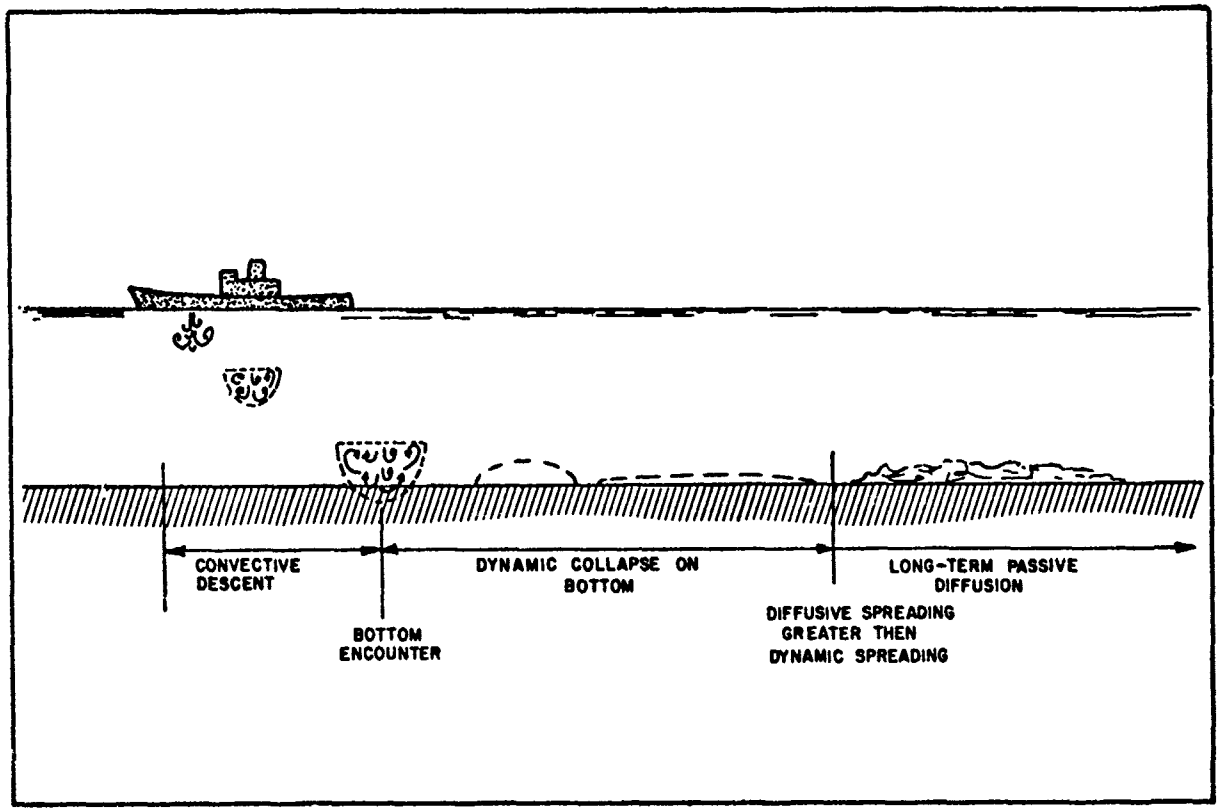

Figure 3. Illustration of idealized bottom encounter after instantaneous dump of dredged material (from Brandsma and Divoky 1976)

Convective descent

17. A single cloud that maintains a hemispherical shape during convective descent is assumed to be released. Since the solids concentration in discharged dredged material is usually low, the cloud is expected to behave as a dense liquid; thus a basic assumption is that a buoyant thermal analysis is appropriate. The equations governing the motion are those for conservation of mass, momentum, buoyancy, each solid, and vorticity. The equations are straightforward statements of conservation principles and are presented by Brandsma and Divoky (1976). It should be noted that the entrainment coefficient associated with the entrainment of ambient fluid into the descending hemispherical cloud is assumed to vary smoothly between its value for a vortex ring and the value for turbulent thermals. Model results are quite sensitive to the entrainment coefficient, which in turn is dependent upon the material

being dumped (the higher the moisture content, the larger the value of the entrainment coefficient).

Dynamic collapse

18. During convective descent, the dumped material cloud grows as a result of entrainment. Eventually, either the material reaches the bottom or the density difference between the discharged material and the ambient fluid becomes small enough for a position of neutral buoyancy to be assumed. In either case, the vertical motion is arrested and a dynamic spreading in the horizontal direction occurs. The basic shape assumed for the collapsing cloud is an oblate spheroid. With the exception of vorticity, which is assumed to have been dissipated by the stratified ambient water column, the same conservation equations used in convective descent but now written for an oblate spheroid are applicable. For the case of collapse on the bottom, the cloud takes the shape of a general ellipsoid and a frictional force between the bottom and collapsing cloud is included.

Long-term transport diffusion

19. The long-term dispersion phase is treated in one of two ways. When the rate of horizontal spreading in the dynamic collapse phase becomes less than an estimated rate of spreading due to turbulent diffusion, the collapse phase is terminated. During collapse, solid particles can settle as a result of their fall velocity. As these particles leave the main body of material, they are stored in small clouds that are characterized by a uniform concentration, thickness, and position in the water column. In the first method of handling the transport-diffusion computations, these small clouds are allowed to settle and disperse until they become large enough to be inserted into the grid positioned in the horizontal plane. Once small clouds are inserted at particular grid points, these points then have a concentration, thickness, and top position associated with them. Figure 4 illustrates a typical concentration profile at a grid point. Computations on the grid are made using a backward convection scheme rather than attempting a numerical solution of the governing convection-diffusion equation. In the backward convection solution technique, a massless particle at each grid point at the present level is moved backward in time by the ambient current to the position it occupied one time-step before. The concentration at the grid point it presently occupies is then taken as a five-point average of points surrounding its old position.

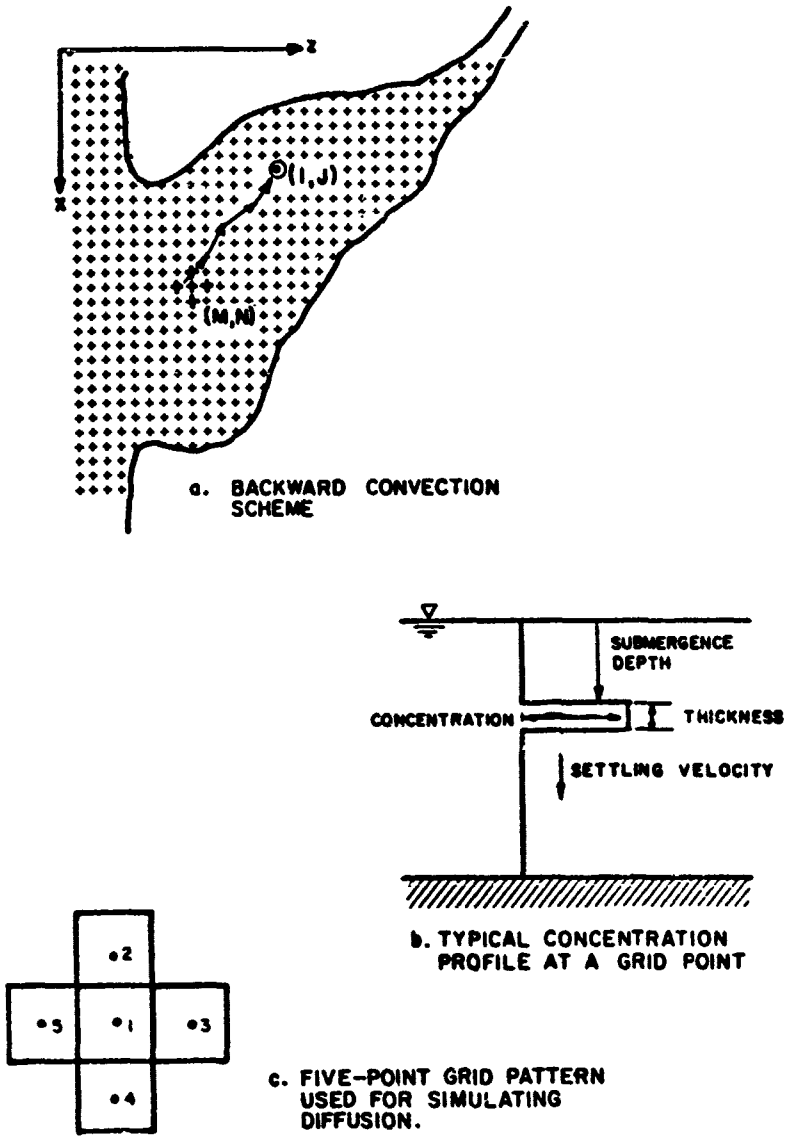

Figure 4. Aspects of passive diffusion
(from Brandsma and Divoky 1976)

20. Rather than making computations at each point of the long-term grid at each time-step, an alternative method for handling the transport-diffusion computations has been incorporated that only uses the horizontal grid for output purposes. The idea for this method was obtained from work by Brandsma and Sauer (1983), on the development of a drilling mud model. Rather than inserting the mass from the previously discussed small clouds into the horizontal grid, each small cloud is assumed to have a Gaussian distribution given by

$$C_c = \frac{m}{(2\pi)^{3/2}\sigma_x\sigma_y\sigma_z} \exp\left[-\frac{1}{2}\left(\frac{(x - x_o)^2}{\sigma_x^2} + \frac{(y - y_o)^2}{\sigma_y^2} + \frac{(z - z_o)^2}{\sigma_z^2}\right)\right] \quad (1)$$

where

x,y,z = spatial coordinates

x_o,y_o,z_o = coordinates of cloud centroid

$\sigma_x,\sigma_y,\sigma_z$ = standard deviations

m = total mass of cloud in ft^3

At the end of each time-step, each cloud is advected horizontally by the input velocity field. The new position of the cloud centroid is determined by

$$x_{o_{new}} = x_{o_{old}} + u \cdot \Delta t$$

$$z_{o_{new}} = z_{o_{old}} + w \cdot \Delta t \quad (2)$$

where

u,w = local ambient velocities, fps

Δt = long-term time-step, sec

21. In addition to advection or transport of the cloud, the cloud grows both horizontally and vertically as a result of turbulent diffusion. The horizontal diffusion is based upon the commonly assumed 4/3 power law. Therefore the diffusion coefficient is given as

$$K_{x,z} = A_L L^{4/3} \quad (3)$$

where A_L is an input dissipation parameter and L is set equal to four standard deviations. The expression for the horizontal growth of a cloud then becomes

$$\sigma_{x,z_{new}} = \sigma_{x,z_{old}}\left[1 + 4^{4/3}\,\frac{2}{3}\,\frac{A_L \Delta t}{\sigma_{x,z_{old}}^{2/3}}\right]^{3/2} \quad (4)$$

22. Vertical growth is similarly achieved by employing the Fickian expression

$$\sigma_y = (2K_y t)^{1/2} \tag{5}$$

where

K_y = vertical diffusion coefficient

t = time since formation of cloud

From Equation 5

$$\frac{d\sigma_y}{dt} = K_y (2K_y t)^{-1/2} = \frac{K_y}{\sigma_y} \tag{6}$$

and thus

$$\sigma_{y_{new}} = \sigma_{y_{old}} + \frac{K_y}{\sigma_{y_{old}}} \Delta t \tag{7}$$

where K_y is a function of the stratification of the water column. The maximum value of K_y is input as a model coefficient and occurs when the water density is uniform.

23. If long-term output is desired at the end of a particular time-step, the concentration of each solid type is given at each grid point by summing the contributions from individual clouds as

$$C_t = (2\pi)^{-3/2} \sum_{i=1}^{N} \left\{ \frac{m_i}{\sigma_{x_i} \sigma_{y_i} \sigma_{z_i}} \exp\left[-\frac{1}{2} \left(\frac{(x - x_{o_i})^2}{\sigma^2_{x_i}} + \frac{(y - y_{o_i})^2}{\sigma^2_{y_i}} + \frac{(z - z_{o_i})^2}{\sigma^2_{z_i}} \right) \right] \right\} \tag{8}$$

where N is the number of small clouds of a particular solid type and y (the vertical position at which output is desired) is specified through input data.

24. At the present time, the effect of horizontal solid boundaries has not been included. Therefore the Gaussian cloud method of transport-diffusion computations should only be used if solid boundaries are far removed from the suspended material. However, such an effect due to the bottom and the water surface has been included in the vertical. This is accomplished through reflection principles by assuming that identical clouds lie above the water surface and below the bottom.

25. In addition to the horizontal advection and diffusion of material, settling of the suspended solids also occurs. Therefore, at each new point the amount of solid material deposited on the bottom and a corresponding thickness

are also determined. A basic assumption in the models is that once material is deposited on the bottom it remains there, i.e., neither erosion nor stable-bed movement of material is allowed. This is the primary theoretical limitation of the models that restricts their usefulness to the study of the short-term fate of discharged material.

Model Capabilities

26. The computer program enables the computation of the physical fate of dredged material disposed in open water. The following discussion describes particular capabilities or special features of the code.

Ambient environment

27. A wide range of ambient conditions is allowed in model computations. Conditions (ranging from those found in relatively shallow and well-mixed bays and estuaries to highly stratified two-layer flow fields found in estuaries where salt wedges are formed) can be variable from one long-term grid cell to the next. The only restriction on bottom topography is that associated with the collapse phase which was discussed in paragraph 13. Any of three options of ambient current illustrated in Figure 5 may be selected, with the simplest case being the time-invariant profiles shown in Figure 5a for a constant depth disposal site. The ambient density profile is input as a function of water depth at the deepest point in the disposal site. This profile may vary with time but is the same at each point of the grid.

Time-varying fall velocities

28. If a solid fraction is specified as being cohesive, the settling velocity is computed as a function of the suspended sediment concentration of that solid type. The following algorithm is currently used

$$V_s = \begin{cases} 0.0017 & \text{if } C \leq 25 \text{ mg/ℓ} \\ 0.00713\, C^{4/3}/304.8 & \text{if } 25 \leq C \leq 300 \text{ mg/ℓ} \\ 0.047 & \text{if } C > 300 \text{ mg/ℓ} \end{cases} \tag{9}$$

where

V_s = settling velocity, fps

C = suspended sediment concentration, mg/ℓ

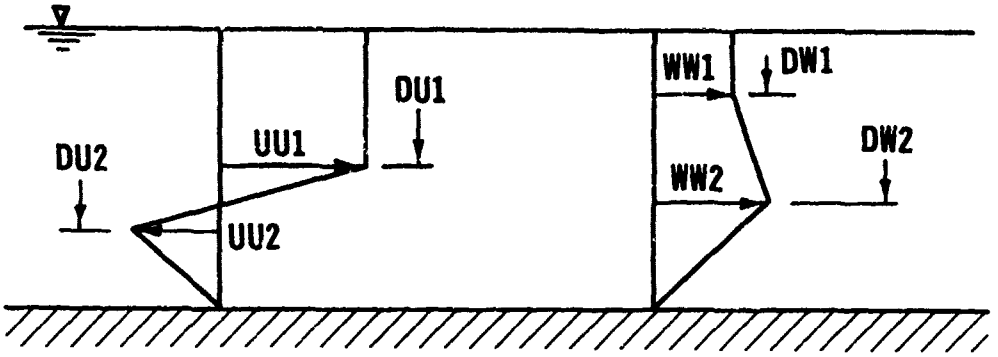

a. SIMPLE ORTHOGONAL VELOCITY PROFILES FOR CONSTANT DEPTH. APPLIED EVERYWHERE IN FIELD

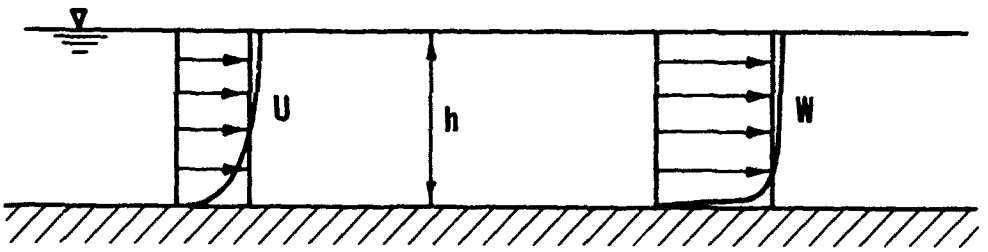

b. VERTICALLY AVERAGED VELOCITY PROFILES FOR VARIABLE DEPTHS WITH EQUIVALENT LOGARITHMIC PROFILES SUPERIMPOSED.

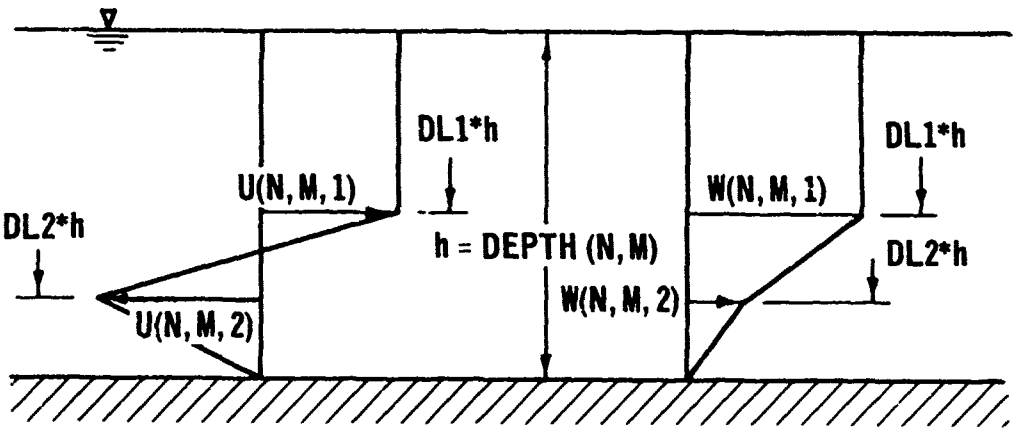

c. TWO-LAYER PROFILES FOR VARIABLE DEPTH

Figure 5. Illustration of the various velocity profiles available for use in models (from Brandsma and Divoky 1976)

Conservative constituent computations

29. The model allows for the dredged material to contain one conservative constituent with a nonzero background concentration of the constituent. Computing the resultant time-history of that concentration provides information on the dilution that can be expected over a period of time at the disposal site.

Output available

30. Through input data, the user specifies the amount of output desired. Much of the input data required, e.g., the water depth field, are immediately printed after being read. At the end of the convective descent phase, the location of the cloud centroid, the velocity of the cloud centroid, the radius of the hemispherical cloud, the density difference between the cloud and the ambient water, the conservative constituent concentration, and the total volume and concentration of each solid fraction are provided as functions of time since release of the material.

31. At the conclusion of the collapse phase, time-dependent information concerning the size of the collapsing cloud, its density, and its centroid location and velocity as well as conservative constituent and solids concentrations can be requested.

32. At various times, as requested through input data, output concerning suspended sediment concentrations and solids deposited on the bottom can be obtained from the transport-diffusion computations. If the backward convection long-term scheme is employed, the suspended sediment concentration and the location of its "top hat" profile (Figure 4) are provided at each grid point for each sediment fraction. However, if the Gaussian cloud long-term scheme is selected, only concentrations at the water depths requested are provided at each long-term grid point. In both cases, the volume of each sediment fraction that has been deposited in each grid cell is provided. At the conclusion of the simulation, a voids ratio specified through input data is used to compute the thickness of the deposited material.

Assembly of Input Data

33. Depending upon the complexity of ambient conditions at the disposal site, the preparation of input data can range from requiring the application of a three-dimensional model to provide stratified velocity fields to a simple

input data setup of perhaps 20 to 25 lines. Input data can be grouped into (a) a description of the ambient environment at the disposal site, (b) characterization of the dredged material, (c) data describing the disposal operation, and (d) model coefficients.

Disposal site data

34. The first task to be accomplished when applying the models is that of constructing a horizontal grid over the disposal site. The number of grid points should be kept as small as possible but large enough to extend the grid beyond the area of interest at the level of spatial detail desired. Quite often one may wish to change the horizontal grid after a few preliminary runs. Water depths and the horizontal components of the ambient current must be input at each grid point. Any of the three options of velocity input illustrated in Figure 5 may be selected, with the simplest case being velocities at a constant depth disposal site. The ambient density profile at the deepest point in the disposal site must also be input. This profile may vary with time but is assumed to be the same at each point of the grid. The grid employed in the study discussed here is presented in Figure 6.

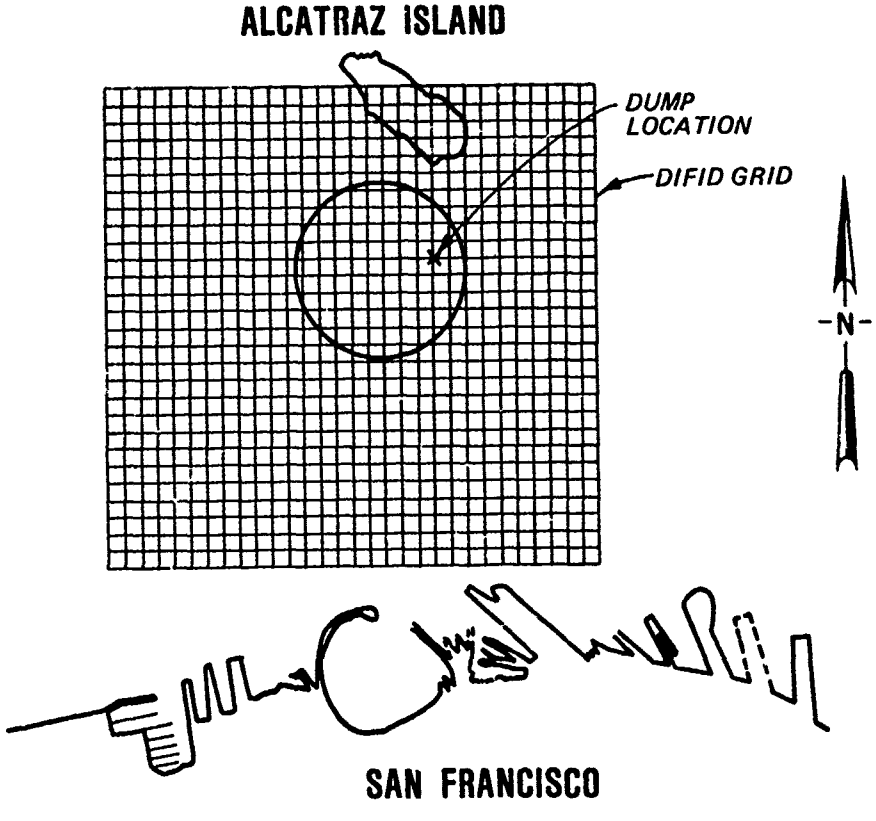

Figure 6. Numerical model grid

Characterization of dredged material

35. The dredged material can be composed of up to 12 solid fractions, a fluid component, and a conservative chemical constituent. For each solid fraction, its concentration by volume, density, fall velocity, voids ratio, and an indicator as to whether or not the fraction is cohesive must be input. Proper material characterization is extremely important in obtaining realistic predictions from the models. If a conservative chemical constituent is to be traced, its initial concentration and a background concentration must be given. In addition, the bulk density and aggregate voids ratio of the dredged material must be prescribed along with its liquid limit.

Disposal operations data

36. Information required includes the position of the barge or scow on the horizontal grid, the volume of material dumped, and the loaded and unloaded draft of the disposal vessel.

Model coefficients

37. There are 14 coefficients in DIFID. Default values are contained in the computer code that reflect the model developer's best guess. However, the user may input other values. Computer experimentation such as that presented by Johnson and Holliday (1978) has shown that results appear to be fairly insensitive to many of the coefficients. The most important coefficients are drag coefficients in the convective descent and collapse phases as well as coefficients governing the entrainment of ambient water into the dredged material cloud.

38. Most coefficients have been set to their default values in the current study. Details of the coefficient values selected are given in Appendix A. The values selected for the entrainment and drag coefficients are based upon experimental work conducted by JBF Scientific Corporation (1978) in which these coefficients are related to the liquid limit of the disposed material.

PART III: TRANSPORT AND RESUSPENSION ANALYSIS

Sand Transport and Resuspension

39. Many empirically based formulas have been developed to study sand transport. They usually involve the difference or ratio between the actual bed shear stress and the critical shear stress at which particle movement begins. In some cases, the shear velocity is used as a measure of shear stress and the ratio of shear velocity to particle fall velocity becomes a measure of the balance of flow strength, represented by shear velocity, against particle resistance to motion represented by particle fall velocity.

40. The formulas are usually known as bed-load formulas, but some appear able to include the suspended-load transport as well. Actually, the transition from bed load to bed load plus suspended load is no more clearly defined than the initial threshhold of motion, and it is possible that one continuous function may well give the total transport rate, including both bed and suspended load. The Ackers-White formula (1973), which is relatively simple to apply, was selected for this study.

41. In the development of the Ackers-White formulation, a coarse sediment is considered to be transported mainly as a bed process and a fine sediment within the body of the flow. Sediment mobility is described by the ratio of the appropriate shear force on unit area of the bed to the immersed weight of a layer of grains. The mobility number is denoted F_{gr} and is defined as:

$$F_{gr} = \frac{v_*^n}{\sqrt{gD(s-1)}} \left[\frac{V}{\sqrt{32} \log\left(\frac{\alpha d}{D}\right)} \right]^{1-n} \tag{10}$$

where

v_* = shear velocity

n = transition exponent depending on sediment size

g = acceleration due to gravity

D = sediment diameter

s = mass density of sediment relative to that of water

V = mean velocity of flow

α = coefficient in rough turbulent equation

d = mean depth of flow

A nondimensional sediment grain size is defined as:

$$D_{gr} = D\left[\frac{g(s-1)}{\nu^2}\right]^{1/3} \qquad (11)$$

where ν = kinematic viscosity of fluid.

42. Once the value of D_{gr} has been derived, the value of n, the transport exponent, can be determined as follows:

for $D_{gr} \leq 1.0$	$n = 1$
for $1.0 < D_{gr} \leq 60$	$n = 1.0 - 0.56 \log D_{gr}$
for $D_{gr} > 60$	$n = 0$

and the value of the sediment mobility number can be calculated from Equation 10.

43. The Ackers-White approach uses dimensionless expressions for sediment transport based on the stream power concept. In the case of coarse sediments, the product of net grain shear and stream velocity as the power per unit area of bed is used, and for fine sediments, the total stream power is used. The dimensionless sediment transport rate, G_{gr}, is described by the equation

$$G_{gr} = C\left(\frac{F_{gr}}{A} - 1\right)^m \qquad (12)$$

where

C = coefficient in sediment transport function

A = value of F_{gr} at nominal initial motion

m = exponent in sediment transport function

The values of C, A, and m can be derived as follows:

for $1 < D_{gr} \leq 60$	$C = 2.86 \log D_{gr} - (\log D_{gr})^2 - 3.53$
	$A = (0.23/\sqrt{D_{gr}}) + 0.14$
	$m = (9.66/D_{gr}) + 1.34$
for $D_{gr} > 60$	$C = 0.025$
	$A = 0.17$
	$m = 1.50$

44. Once the dimensionless sediment transport rate has been derived from

Equation 12, the sediment transport in mass flux per unit mass flow rate, X , can be determined from the equation

$$X = \frac{G_{gr}\, sD}{d}\left(\frac{V}{V_*}\right)^n \tag{13}$$

Silt and Clay Erosion

45. Quantification of erosion rates of silt-clay sediments is difficult in view of the many variables involved, such as the chemical characteristics of the material, the degree of consolidation, armoring, and the physical and chemical properties of the water.

46. An equation based on work by Parthenaides (1962) was used to estimate the subsequent erosion and resuspension of clay and silt which settled to the bottom. The same equation with different coefficients was used to estimate erosion of both relatively unconsolidated clay-silt and clumps of consolidated clay-silt that result from clamshell dredging operations.

47. Small-scale laboratory experiments indicate that partially consolidated cohesive material is eroded in direct proportion to applied shear stresses and that the process is independent of suspended load concentration. In equation form this relationship, referred to as the modified Parthenaides equation, is

$$\frac{dm}{dt} = M\left(\frac{\tau}{\tau_c} - 1\right) \tag{14}$$

where

$\frac{dm}{dt}$ = mass of sediment removed per unit bed area per unit time

M = constant with units of mass per unit bed area per unit time

τ = bottom shear stress

τ_c = critical shear stress for erosion

48. The constant M is a function of the degree of consolidation of the bed and erosion depth within the deposit. A typical value for partially unconsolidated clay sediment would be around 0.002 $kg/m^2/sec$.

PART IV: TEST PROGRAM AND RESULTS

Test Conditions

Currents

49. Disposal site currents collected on the San Francisco Bay-Delta physical model for five different hydrodynamic conditions were used for this study (Tetra Tech 1984). The six hydrodynamic conditions tested in the physical model were as follows:

Series	Tide Range	Delta Net Outflow, cfs
11	19-year mean	4,400
12	19-year mean	40,000
21	Neap	4,400
22	Neap	40,000
31	Spring	4,400
32*	Spring	40,000

* Physical model data unavailable for this study.

50. The physical model testing included both the bathymetric condition that existed at the disposal site prior to the depth loss and the bathymetric condition recently observed in which a mound had developed at the disposal site, resulting in significant loss of depth. The mound-out condition had a depth of 160 ft at the disposal site, while the mound-in condition had a depth of only 29 ft. The mound-in currents from the physical model study, shown in Figure 7, were used as input to DIFID in this effort, since the bottom contours are the same except that the mound peak was excavated to 40 ft deep for the DIFID runs.

51. In order to evaluate the sensitivity of the site's dispersive capability to the current environment, another current condition was tested. This additional test, which is referred to as Series XX, was simply the currents from Series 11 multiplied by an arbitrarily selected two-thirds factor. Series XX had maximum near-surface ebb currents of 4.2 fps and maximum flood currents of 2.9 fps.

Disposal material

52. Based on information from the San Francisco District, the material simulated in the barge dump consisted of 60 percent clay-silt ranging in size

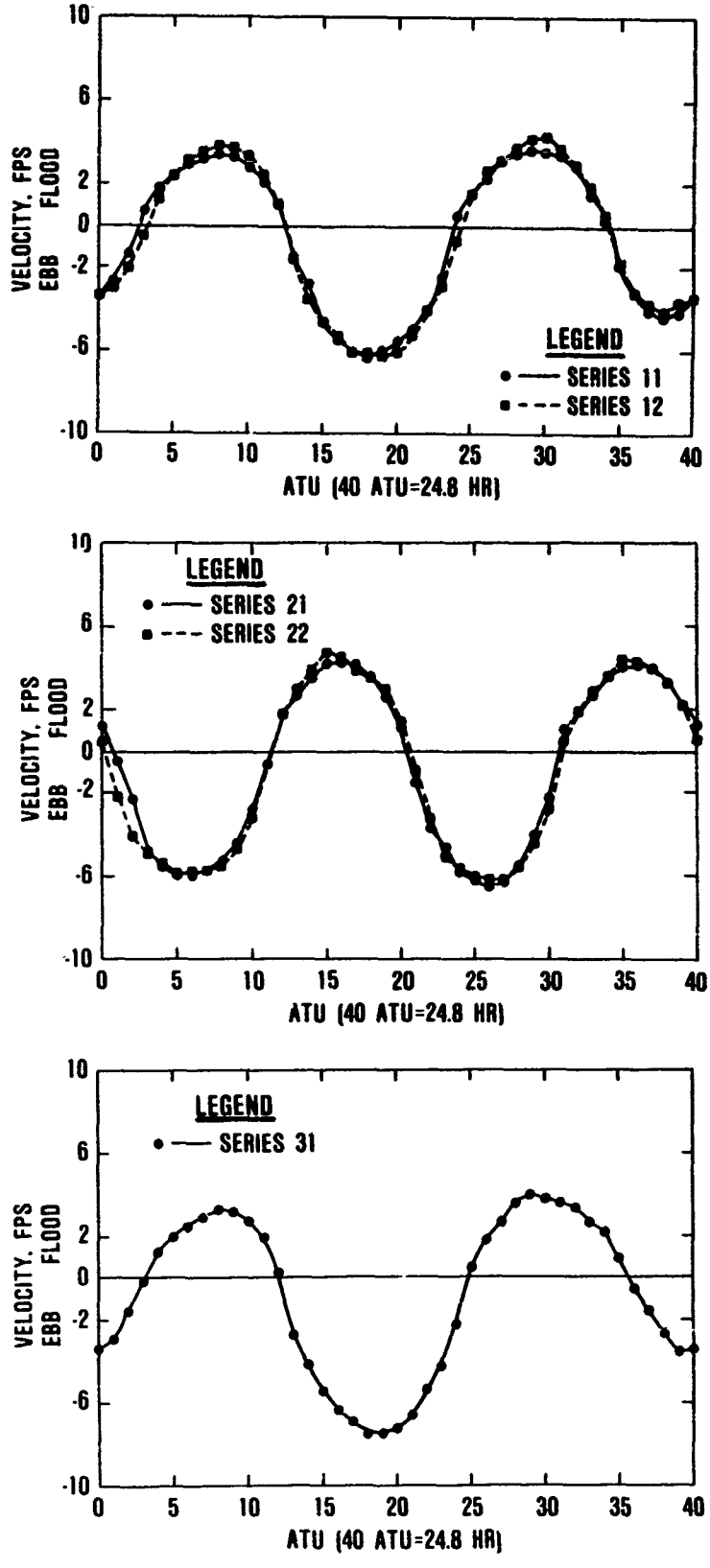

Figure 7. Near-bottom velocities measured at the mound in the San Francisco Bay-Delta model

from 0.02 to less than 0.002 mm and 40 percent fine sand ranging in size from 0.2 to 0.06 mm. The bulk density of the barge slurry was 1.44 g/cc, resulting in a moisture content for the slurry of about 74 percent. Testing included a slurry with no clumps to simulate barge material obtained from a hydraulic dredging operation and a slurry in which 30 percent of the clay-silt fraction was in the form of clumps or clods to simulate barge material from a clamshell or bucket dredging operation.

53. In order to evaluate the effect of bulk density on initial deposition of the dumped material, simulations were also conducted using bulk densities of 1.2, 1.3, 1.6, and 1.7 g/cc.

Dump location

54. The location of the dump for all simulations discussed in this report is directly above the mound, as shown in Figure 6. Results from this report can only be applied to material dumped at that location within the disposal site.

Dump time

55. All dump simulations were made at about strength of ebb. The duration of each simulation was about 15 min. Dumps made at other times during the tidal cycle would have resulted in larger amounts of material being initially deposited within the Alcatraz disposal site limits.

Dump size

56. To be representative of a typical barge, the dump size selected for testing was 1,000 cu yd. In order to investigate larger dump sizes, a limited number of tests included dumps of 2,000 and 3,000 cu yd.

Discussion of Results

Dump simulation

57. The dump model estimated deposition of material within the designated disposal site and on the mound for five hydrodynamic conditions (Series 11, 12, 21, 22, and 31). The primary dump size was 1,000 cu yd and the bulk density was 1.44 g/cc in the disposal of 2,852 cu ft of sand and 4,278 cu ft of clay-silt, the remainder of the 1,000 cu yd being water. The dump location was directly over the mound, and the dump time during the tidal cycle was at maximum ebb for each of the five conditions. Details of the model input and output (DIFID) from the dump simulations and sample results are given in

Appendix A. The initial deposition of each fraction of material (in cubic feet and percent) from a 1,000-cu-yd maximum ebb dump at the mound and within the site tested is tabulated as follows:

Series	Within Site Sand	At Mound* Sand	Within Site Silt-Clay	At Mound* Silt-Clay	Within Site Clumps	At Mound* Clumps
			In Cubic Feet			
No Clumps						
11	711	498	643	500	NA	NA
12	825	530	639	503	NA	NA
21	762	477	560	495	NA	NA
22	820	521	646	503	NA	NA
31	577	344	287	224	NA	NA
30 Percent Clumps						
11	711	498	311	215	1,284	1,284
12	826	531	359	226	1,284	1,284
21	670	477	249	205	1,284	1,284
22	820	521	320	223	1,284	1,284
31	501	344	255	145	1,266	1,120
			In Percent			
No Clumps						
11	25	17	15	12		NA
12	29	19	15	12		NA
21	27	17	13	12		NA
22	29	18	15	12		NA
31	20	12	7	5		NA
30 Percent Clumps						
11	25	17	10	7	100	100
12	29	19	12	8	100	100
21	23	17	11	7	100	100
22	29	18	11	7	100	100
31	18	12	9	5	99	87

* Mound area defined as area with depths of 40 ft mllw.

58. In addition to the tests using 1.44 g/cc bulk density, tests with Series 11 conditions were also conducted using bulk densities of 1.2, 1.3, 1.6, and 1.7 g/cc (Figure 8) to determine the impact of varying bulk density on the percent of material deposited within the disposal site limits.

59. In addition to the 1,000-cu-yd dump size, some limited testing with Series 11 and 31 conditions was conducted using 2,000- and 3,000-cu-yd dumps. The effect of varying dump size on the amount of material deposited within the

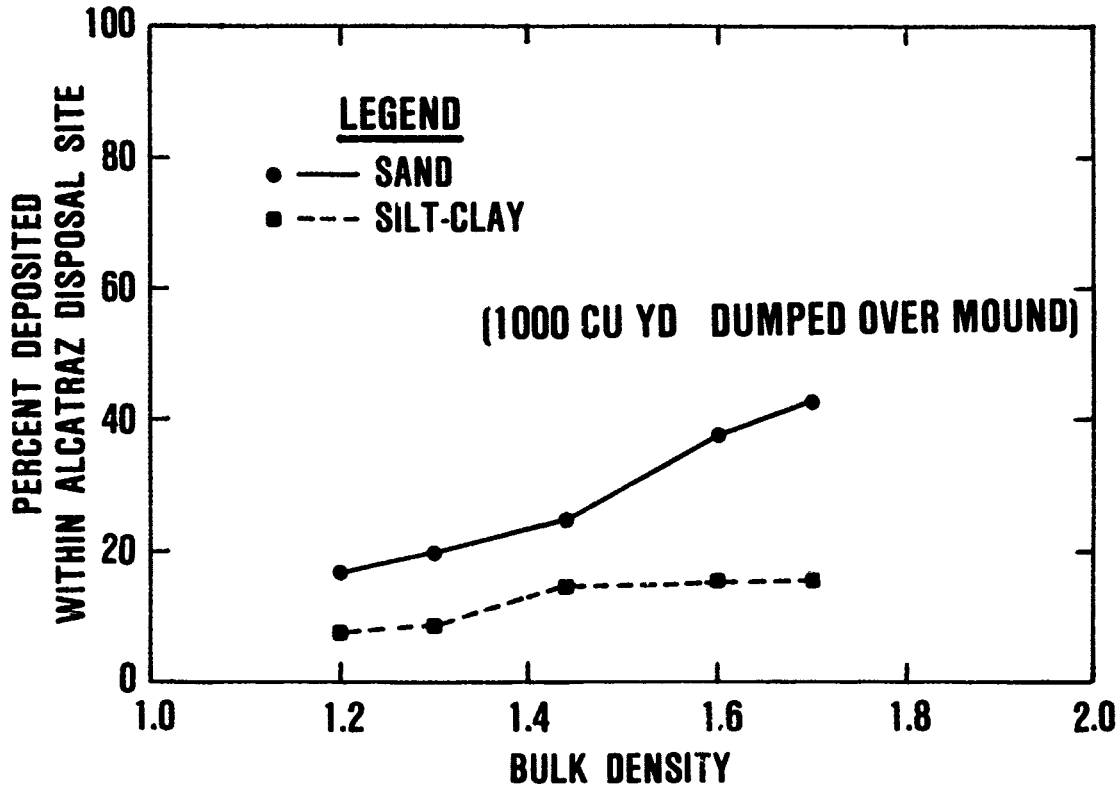

Figure 8. The impact of bulk density on the percent of material deposited within the Alcatraz site

disposal site is shown in Figures 9 and 10. Results show that in the 1,000- to 3,000-cu-yd dump size range the relation is basically linear. For example, increasing the dump size from 1,000 to 3,000 cu yd resulted in roughly a threefold increase in material deposited.

Sand transport

60. Based on the Ackers-White (1973) transport formula for the sand fraction of the dumped material, the transport potential on the mound in 40 ft of water for each condition is given in the following tabulation in pounds per tidal cycle per foot of width. Details of the calculations are given in Appendix B.

Series	Transport Potential (lb/tidal cycle/ft width)
11	28,200
12	33,600
21	51,800
22	46,900
31	75,000
XX	2,600

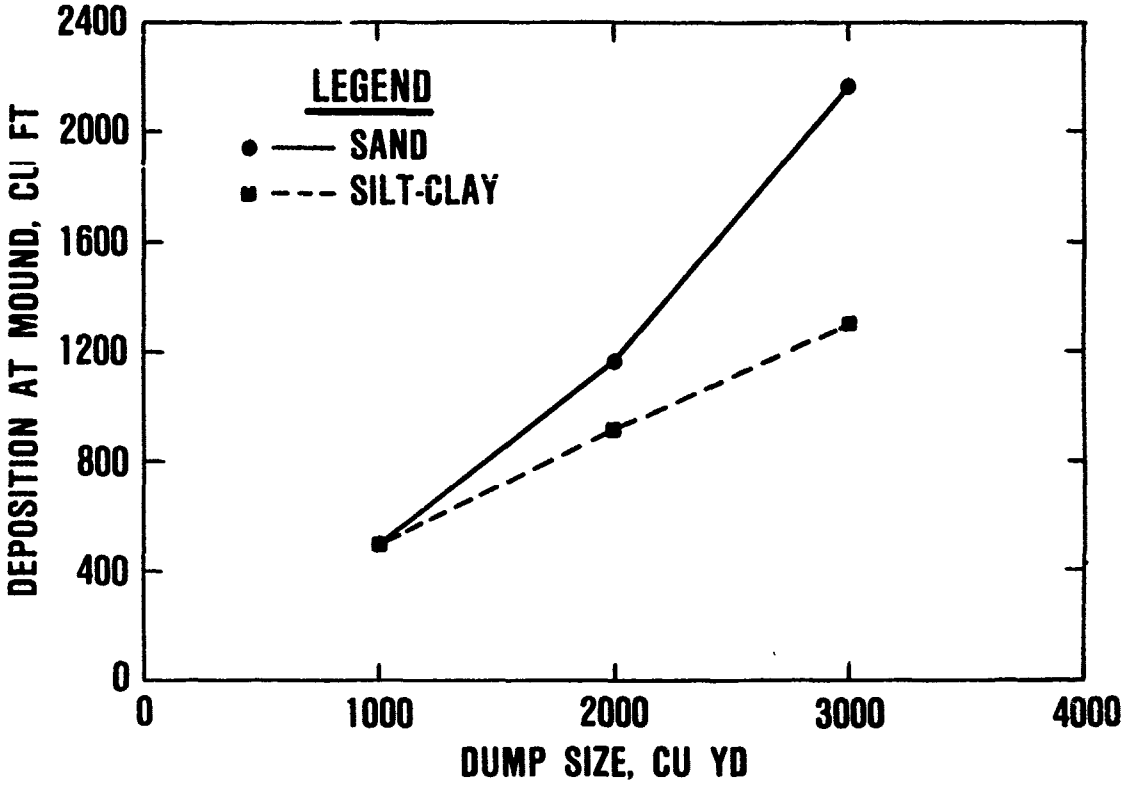

Figure 9. Effect of dump size on the amount of material deposited within the Alcatraz site (Series 11)

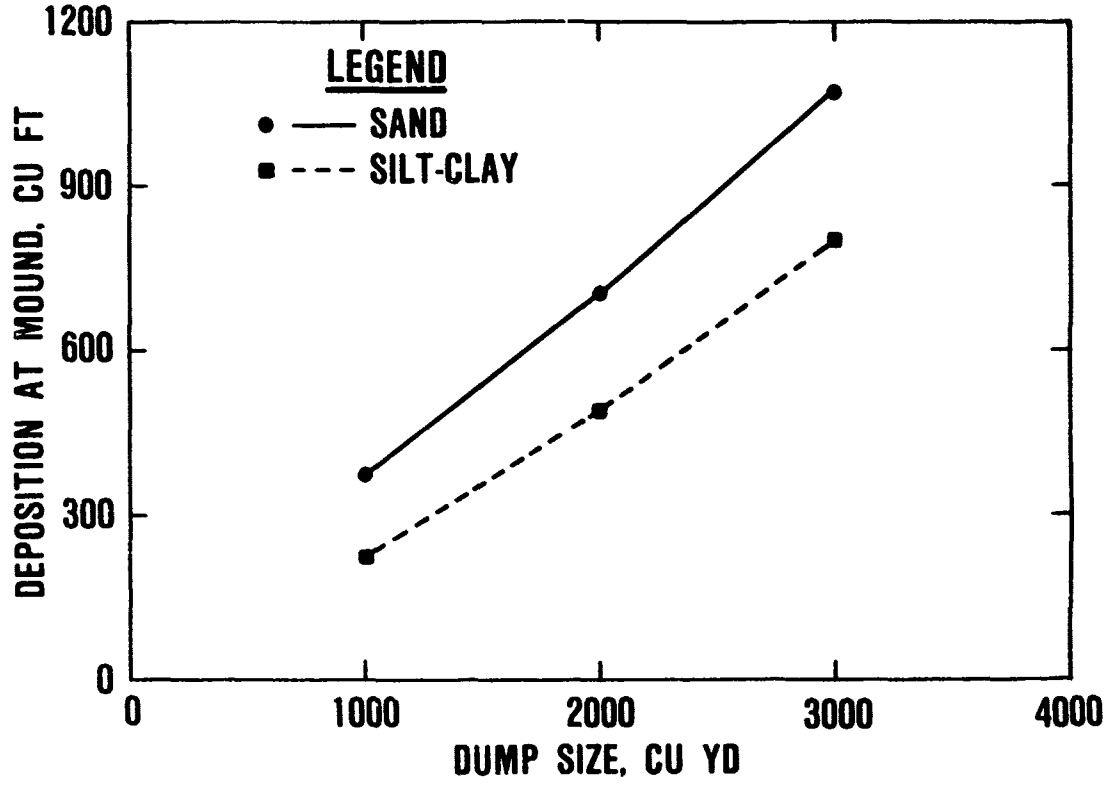

Figure 10. Effect of dump size on the amount of material deposited within the Alcatraz site (Series 31)

61. Since the width of the mound transverse to flow in 40 ft of water was estimated to be about 400 ft (Figure 2), the transport potential from the mound for Series 11, 12, 21, 22, and 31 are 11, 13, 21, 19, and 30 million lb of sand per tidal cycle, respectively. Transport potential for Series XX (which arbitrarily reduced Series 11 velocities by one-third) is reduced to 0.8 million lb of sand per tidal cycle.

Clay-silt erosion

62. Based on the Parthenaides equation for the clay-silt fraction of the dumped material, the erosion rate potential on the mound in 40 ft of water for each condition for both unconsolidated and consolidated material is given in the following tabulation in pounds per tidal cycle per square foot of bottom. Details of the calculations are given in Appendix C.

Series	Erosion Potential (lb/tidal cycle/sq ft)	
	Unconsolidated	Clumps
11	363	3.4
12	390	4.2
21	497	7.2
22	508	8.0
31	462	6.8
XX	140	0.4

63. Since the bottom area of the mound in 40 ft of water is estimated to be about 160,000 sq ft, the erosion potential on the mound for Series 11, 12, 21, 22, and 31 are 58, 62, 80, and 74 million lb of clay-silt per tidal cycle, respectively, for the unconsolidated clay-silt and 0.5, 0.7, 1.2, 1.3, and 1.1 million lb of clay-silt per tidal cycle, respectively, for the clumps. For Series XX the transport potential for unconsolidated clay-silt is 22 million lb per tidal cycle and for consolidated clay-silt only about 0.1 million lb per tidal cycle.

PART V: CONCLUSIONS

64. The conclusions reached as a result of this study of maximum ebb dumps are summarized as follows:

a. Based on the maximum ebb dump simulations, significant amounts of the dredged material (both sand and clay-silt) actually are initially deposited within the disposal site limits.

b. Based on the tidal currents indicated by the physical model and the estimated erosion potential, the Alcatraz disposal site is capable of dispersing unconsolidated clays and silts of the magnitude presently being dumped.

c. Based on the tidal currents indicated by the physical model and the estimated transport potential, the capability at the mound location to transport fine sands from the mound is considerable, averaging about 40,000 cu yd of fine sand per tidal cycle.

d. Based on tidal currents indicated by the physical model, the site's capability to erode consolidated clay-silts in the form of clumps, which can result from clamshell dredging, is much less than the volume of clumps that can be disposed during a dredging operation. The result of dumping a large volume of clumps over a short period of time at the location tested would be significant mounding. Consolidation and armoring of the mound over time would further increase its resistance to erosion.

REFERENCES

Ackers, P., and White, W. R. 1973 (Nov). "Sediment Transport: New Approach and Analysis," Journal, Hydraulics Division, American Society of Civil Engineers, No. HY11.

Brandsma, M. G., and Divoky, D. J. 1976 (May). "Development of Model for Prediction of Short-Term Fate of Dredged Material Discharged in the Estuarine Environment," Contract Report D-76-5, US Army Engineer Waterways Experiment Station, Vicksburg, Miss.

Brandsma, M. G., and Sauer, T. C., Jr. (1983). "Mud Discharge Model-Report and User's Guide," Exxon Production Research Company, Houston, Tex.

JBF Scientific Corporation. 1978 (Sep). "Calibration of a Predictive Model for Instantaneously Discharged Dredged Material," R-804994, Wilmington, Mass.

Johnson, B. H. "User's Guide for Dredged Material Disposal Models for Computing the Short-Term Fate at Open-Water Sites" (in preparation), US Army Engineer Waterways Experiment Station, Vicksburg, Miss.

Johnson, B. H., and Holliday, B. W. 1978 (Aug). "Evaluation and Calibration of the Tetra Tech Dredged Material Disposal Models Based on Field Data," Technical Report D-78-47, US Army Engineer Waterways Experiment Station, Vicksburg, Miss.

Koh, R. C. Y., and Chang, Y. C. 1973 (Dec). "Mathematical Model for Barged Ocean Disposal of Waste," Environmental Protection Technology Series EPA 660/2-73-029, US Environmental Protection Agency, Washington, DC.

Parthenaides, E. 1962. A Study of Erosion and Deposition of Cohesive Soils in Salt Water, Ph. D. Dissertation, University of California, Berkeley, Calif.

Tetra Tech. 1984 (Feb). "Report on the Study of Currents at the Alcatraz Disposal Site, San Francisco Bay-Delta Model," Draft Report, prepared for US Army Engineer District, San Francisco, Calif.

APPENDIX A: DIFID INPUT AND OUTPUT

Input

1. The description of the ambient environment includes the depth and tidal currents at each point within the model. The depths at each grid point are shown on the depth grid map in Figure A1. The velocity at each grid point was generated from the physical model velocity measured above the mound.

2. The characterization of the dredged material includes for each solid fraction its concentration by volume, density, fall velocity, voids ratio, as well as aggregate voids ratio and bulk density. The values used in the Alcatraz simulation are given in Table A1.

3. The disposal operations data include the position of the barge on the horizontal grid, the radius of the initial hemispherical cloud, the depth below the water surface at which the material is released, and the initial velocity of the cloud. For the Alcatraz simulation (1,000-cu-yd dump), the position of the barge on the horizontal grid is shown in Figure A2. The initial cloud radius corresponding to a 1,000-cu-yd dump was 23.45 ft. The depth below the water surface at which the material was released was 8.8 ft. The initial cloud velocity was 5.03 fps downward.

4. The model coefficients used in the Alcatraz study, as well as the default values, are given in Table A2.

Output

5. The duration of the DIFID simulation for all series (11, 12, 21, 22, and 31) was about 1,000 sec. Output included both the deposition pattern of sand and clay-silt and the dispersal of suspended material within the modeled area. As an example, the bottom deposition and suspended sediment dispersal patterns, 1,020 sec after the dump, for the Series 11 ebb current simulation using specified dredged material with no clumps are shown in Figures A3-A5. The bottom deposition and suspended sediment dispersal patterns 1,020 sec after the dump for a Series 11 ebb current simulation using the specified dredged material with 30 percent of the clay-silt fraction introduced as clumps are shown in Figures A6-A9.

Table A1

Characterization of the Dredged Material

	No Clumps	30% Clumps
Sand content by volume, cu ft/cu ft	0.1056	0.1056
Silt-clay content by volume, cu ft/cu ft	0.1584	0.1109
Clumps content by volume, cu ft/cu ft	--	0.0475
Sand density, g/cc	2.60	2.60
Silt-clay density, g/cc	2.60	2.60
Clumps density, g/cc	--	2.60
Fluid density, g/cc	1.018	1.018
Sand fall velocity, fps	0.065	0.065
Silt-clay fall velocity, fps	0.026	0.026
Clumps fall velocity, fps	--	0.50
Sand voids ratio	0.80	0.80
Silt-clay voids ratio	0.80	0.80
Clumps voids ratio	--	0.90
Bulk density, g/cc	1.436	1.436
Aggregate voids ratio	0.80	0.80

Table A2

Values for Model Coefficients

Coefficient	Description	Default Value	Value Used
σ_o	Convective descent entrainment	0.235	0.275
β	Settling coefficient	0.0	0.0
CM	Apparent mass coefficient	1.0	0.40
CD	Drag coefficient of sphere	0.50	0.40
δ	Relates cloud dens. grad. to ambient dens. grad.	0.25	0.25
CDRAG	Drag coefficient of ellipsoid	1.0	0.50
CFRIC	Skin friction of ellipsoid	0.01	0.01
CD3	Drag coefficient of ellipsoidal wedge	0.10	0.10
σ_c	Collapse entrainment coefficient	0.02	0.02
FRICTN	Bottom friction coefficient	0.01	0.01
FI	Modification factor in bottom friction force	0.10	0.10
ALAMDA	Dissipation parameter	0.005	0.005
AKYØ	Max value of vertical diffusion coefficient	0.05	0.05

DEPTH GRID IN FEET

57	51	53	54	59	60	62	64	61	65	69	65	60	65	64	62	47	51	55	40	40	40	60	100
51	52	52	55	64	64	66	67	70	74	79	73	76	78	84	88	98	106	105	84	80	62	84	96
55	54	58	59	67	66	68	74	79	82	87	85	90	99	104	111	119	107	97	85	73	78	87	85
52	55	60	64	67	70	74	80	83	90	93	102	104	101	101	105	115	102	40	40	40	55	69	80
54	56	61	64	71	75	80	83	87	92	99	106	101	96	96	99	91	76	40	40	40	47	59	71
57	59	67	70	74	77	82	88	92	96	103	102	98	92	92	88	76	60	40	40	40	40	43	48
59	65	68	72	74	79	84	88	93	96	102	106	88	84	82	79	67	61	53	47	50	55	57	62
64	67	69	73	77	80	84	87	93	96	100	102	82	75	73	71	68	67	68	66	66	68	74	83
66	67	69	73	76	82	85	88	93	96	98	102	81	74	70	69	68	66	71	77	82	80	86	94
69	71	74	77	79	83	86	87	92	94	97	100	85	84	77	72	71	73	79	82	86	90	90	84
70	72	74	76	77	83	85	87	92	93	96	98	88	88	87	81	82	85	86	87	89	89	84	81
70	73	75	77	79	82	85	87	92	93	95	98	90	90	90	87	87	86	87	88	86	84	83	77
70	72	73	75	76	80	83	85	89	90	93	93	94	96	97	96	96	94	92	88	85	82	75	69
70	73	75	78	80	81	86	86	88	91	92	93	91	92	92	90	94	87	86	81	83	78	68	60
72	73	71	75	76	80	82	84	87	87	85	87	91	90	89	87	84	80	78	80	71	66	57	60
72	73	74	75	76	81	82	82	84	86	83	81	83	83	80	77	75	73	72	70	60	55	55	60
75	76	77	78	79	82	80	78	83	80	80	82	77	76	74	73	72	68	65	58	50	52	57	62
73	74	75	76	77	79	81	80	79	78	78	77	72	72	68	63	65	51	50	47	52	54	54	60
73	74	75	76	77	79	81	80	79	78	78	77	72	72	69	63	50	45	47	48	51	51	53	53
64	66	68	70	72	74	73	71	71	67	56	67	54	51	47	44	43	44	46	47	49	48	48	47
61	64	66	68	70	70	68	65	57	55	54	52	50	48	44	40	42	43	44	45	46	47	46	47
57	57	56	56	56	56	57	53	51	50	48	46	45	43	42	39	42	42	43	42	46	46	46	47
55	54	53	53	51	49	49	44	45	44	43	42	41	40	40	41	41	42	41	42	44	44	47	50
49	48	48	47	46	45	44	42	41	41	40	40	40	40	40	40	40	40	42	46	43	44	49	52
47	46	45	44	43	41	40	40	40	40	40	40	40	40	40	40	40	40	40	40	40	40	40	40

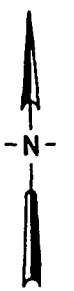

Figure A1. DIFID depth grid in feet ("x" indicates dump location)

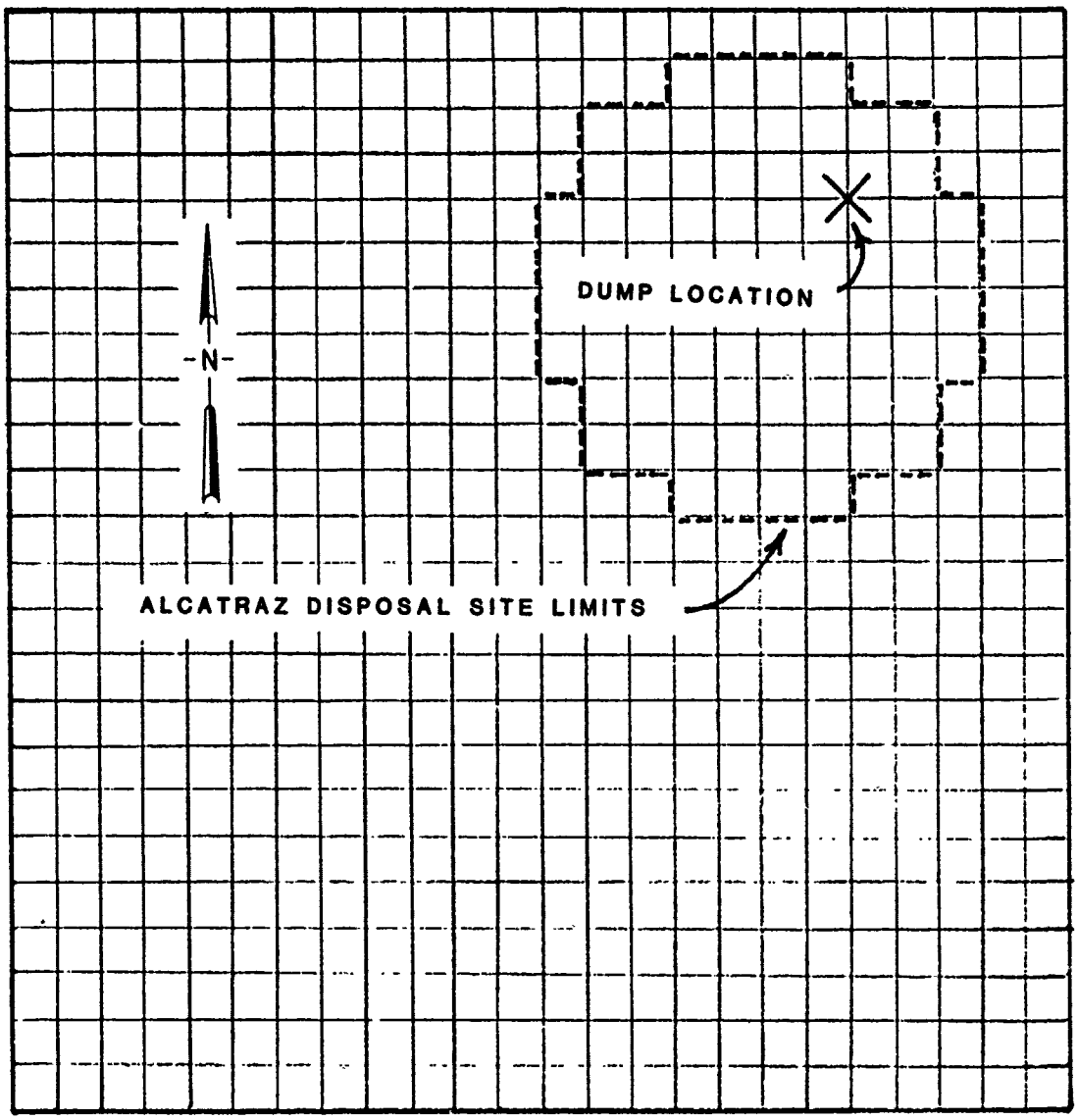

Figure A2. Location of dump on horizontal grid (indicated by "x")

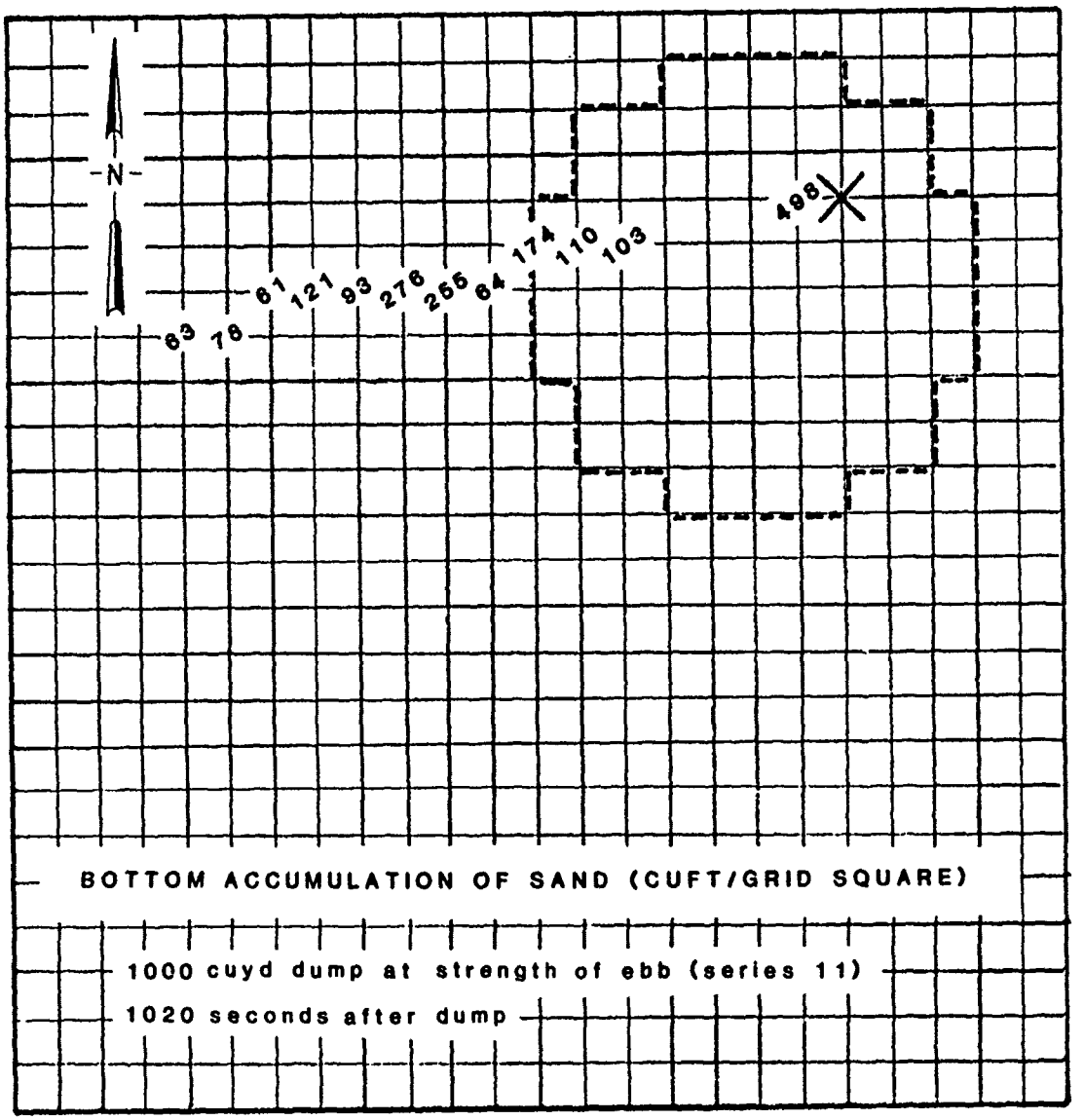

Figure A3. Bottom accumulation of sand for dump of dredged material with no clumps

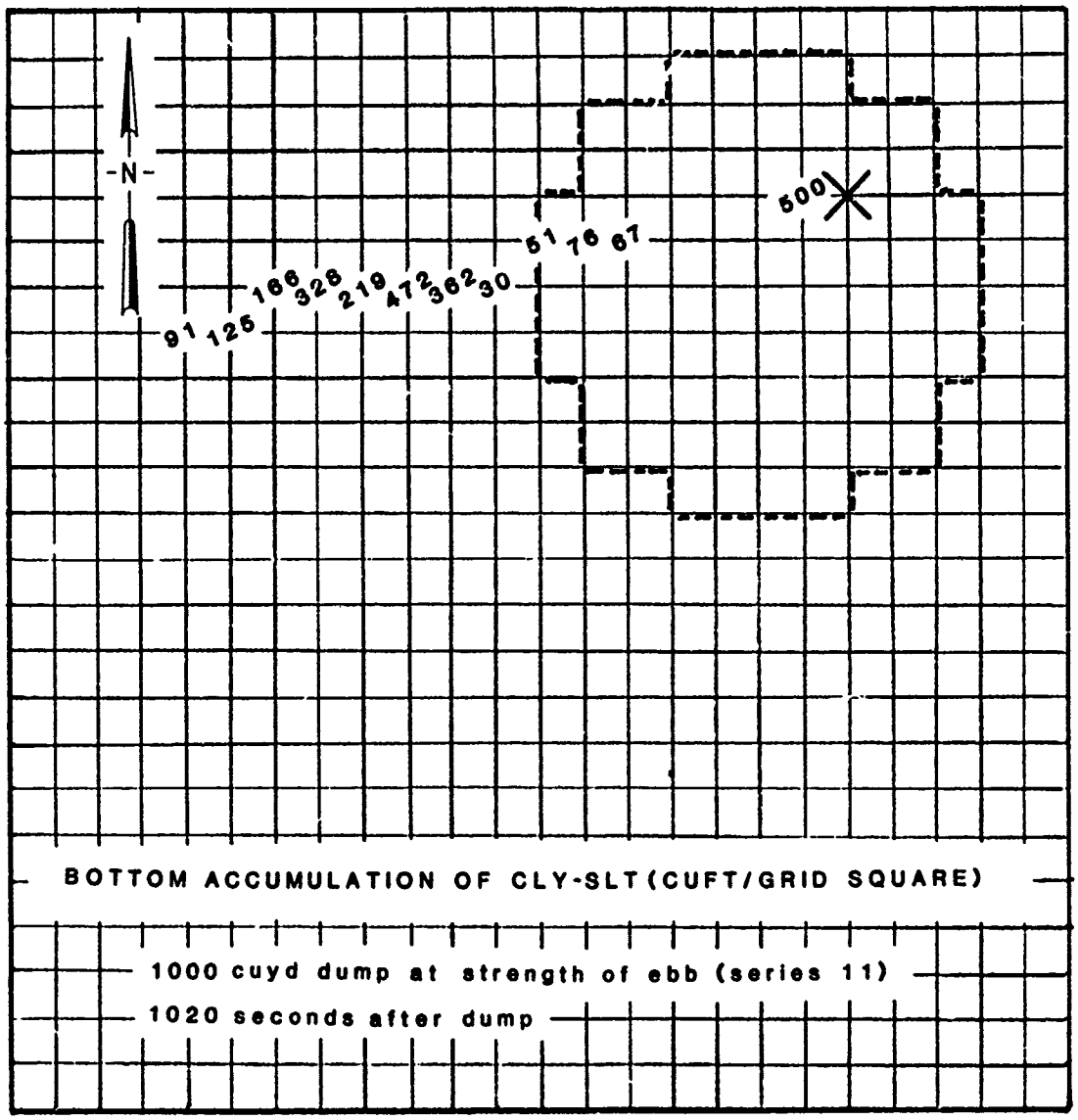

Figure A4. Bottom accumulation of clay-silt for dump dredged material with no clumps

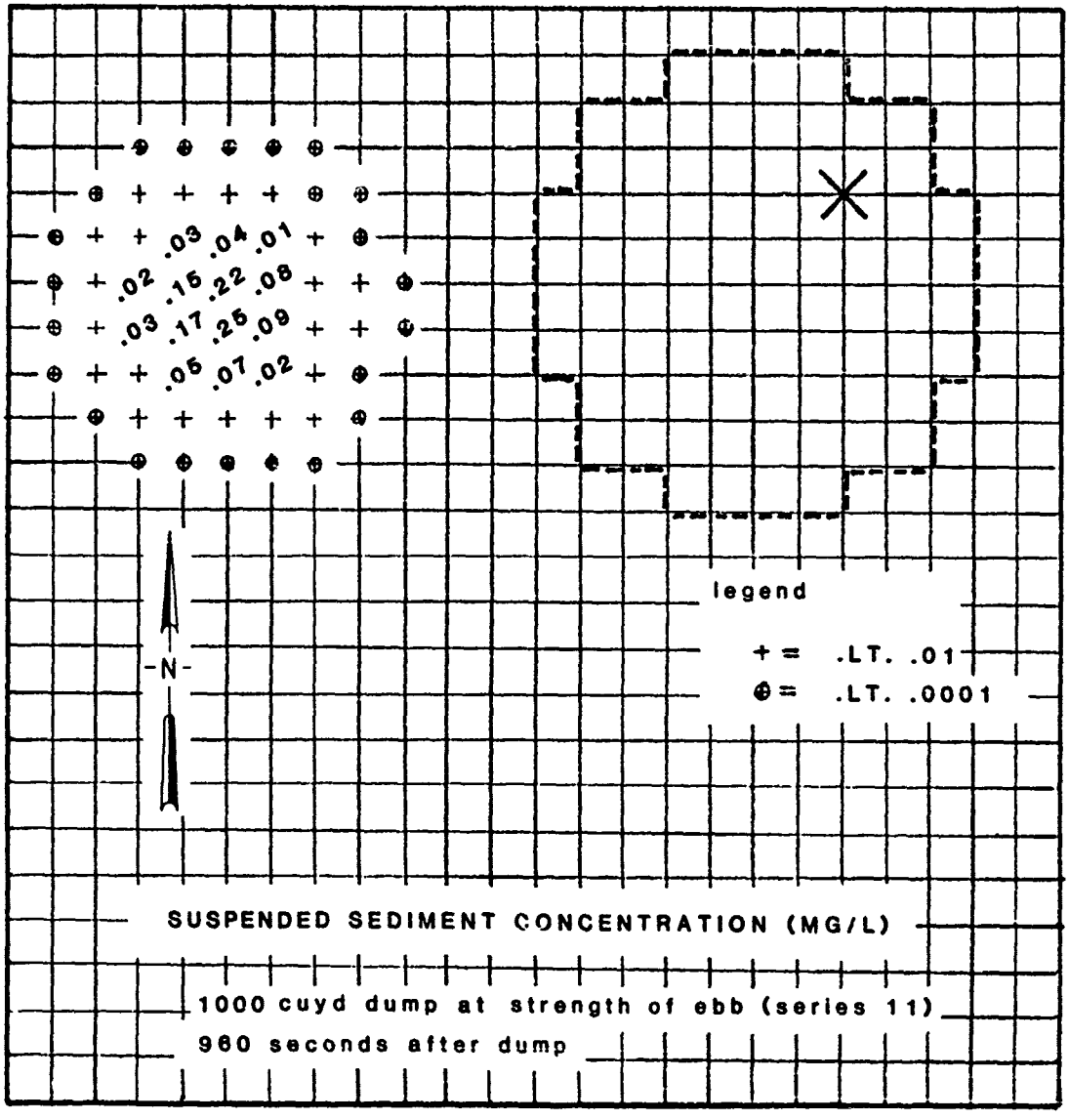

Figure A5. Suspended sediment concentration from dump of dredged material with no clumps

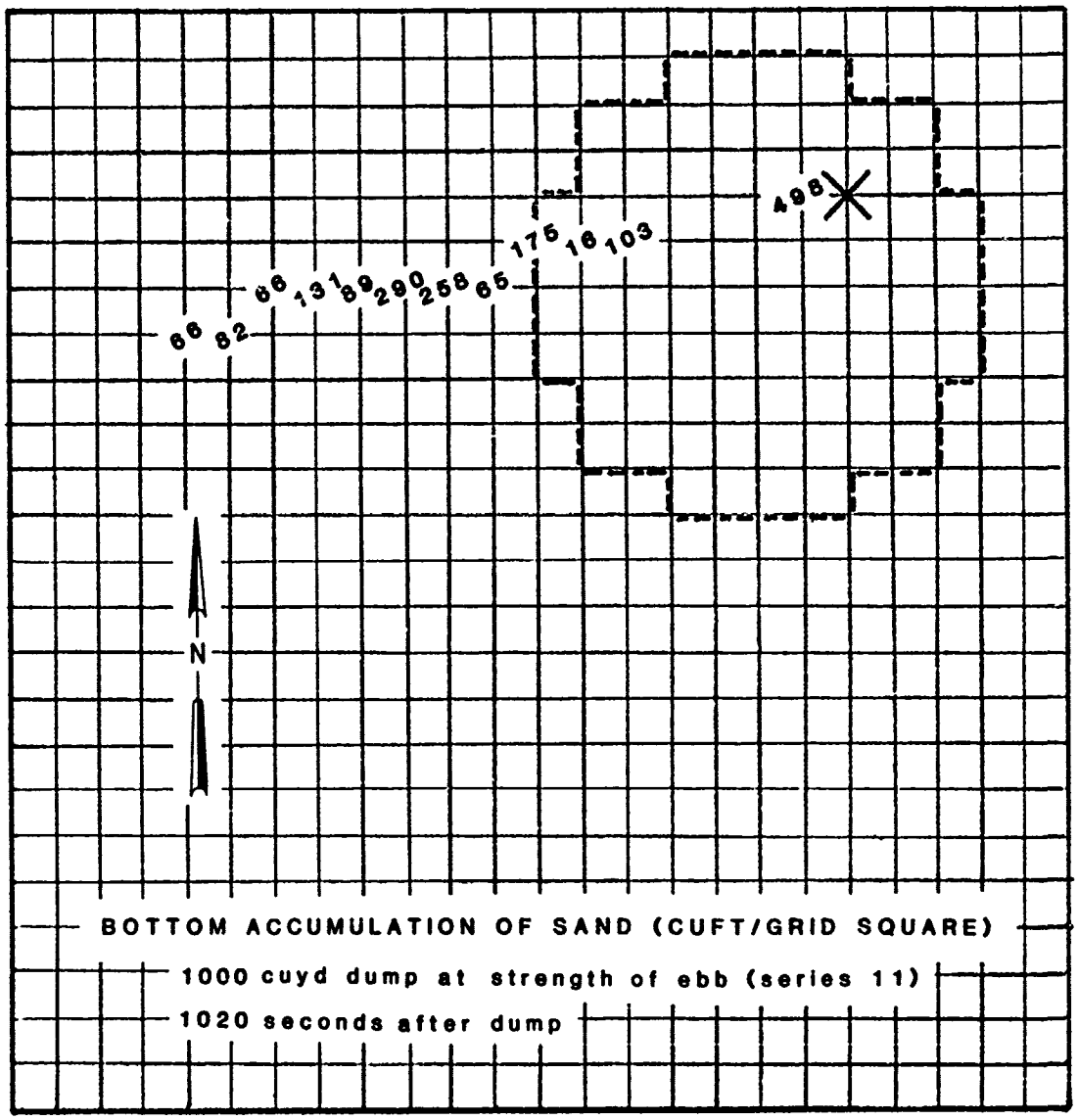

Figure A6. Bottom accumulation of sand from dump of dredged material with 30 percent of clay-silt fraction as clumps

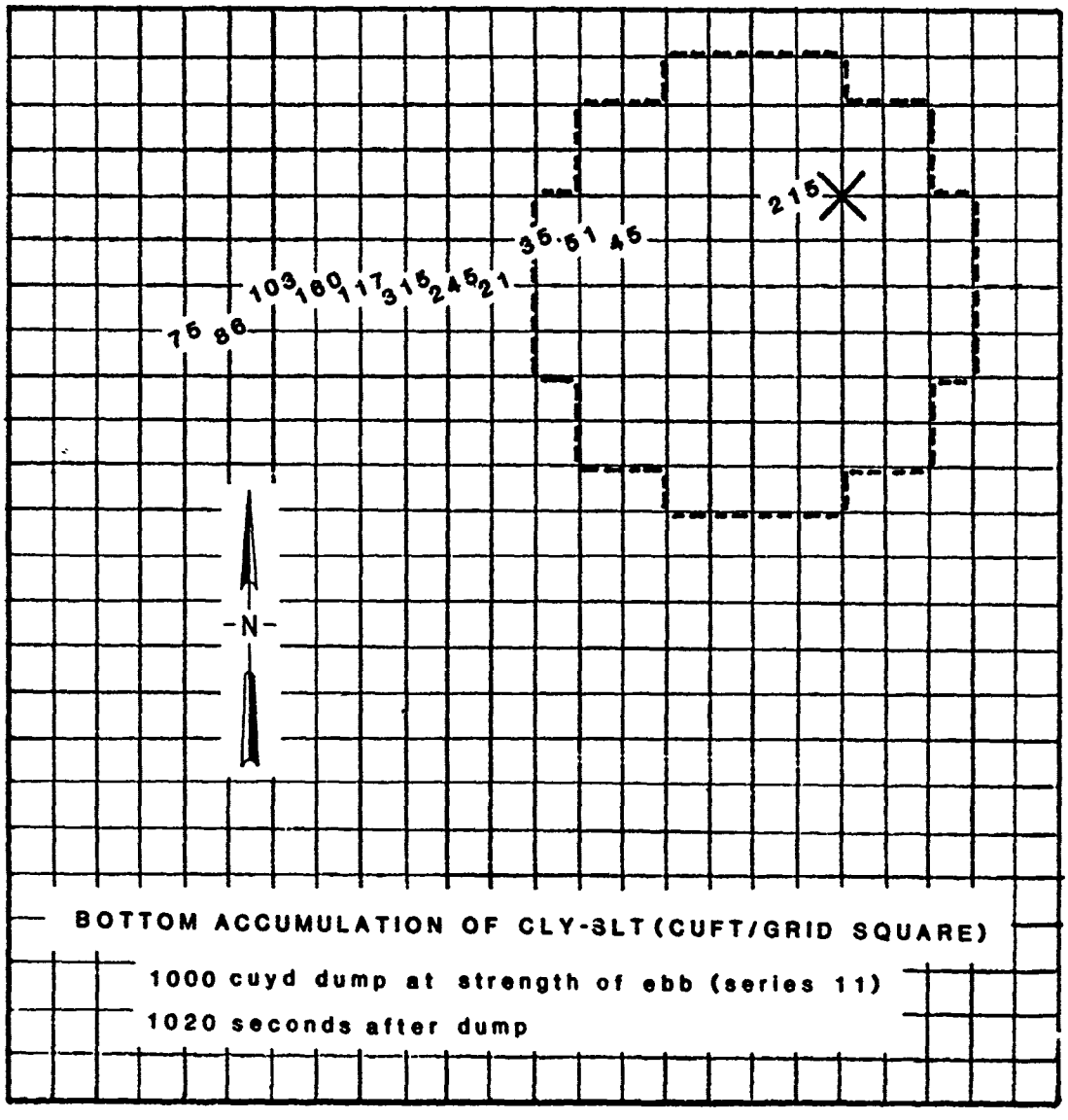

Figure A7. Bottom accumulation of sand from dump of dredged material with 30 percent of clay-silt fraction as clumps

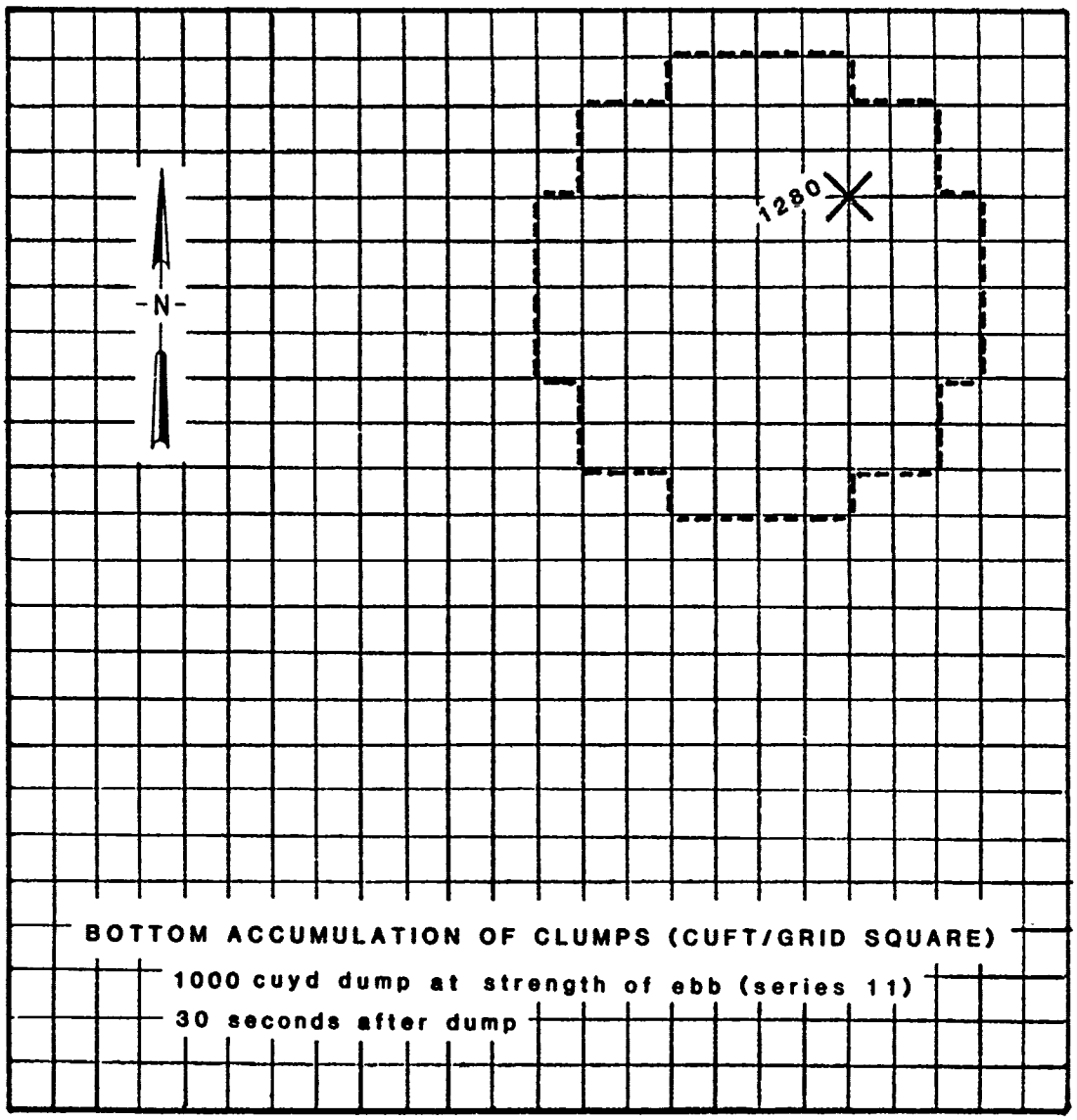

Figure A8. Bottom accumulation of clumps from dump of dredged material with 30 percent of clay-silt fraction as clumps

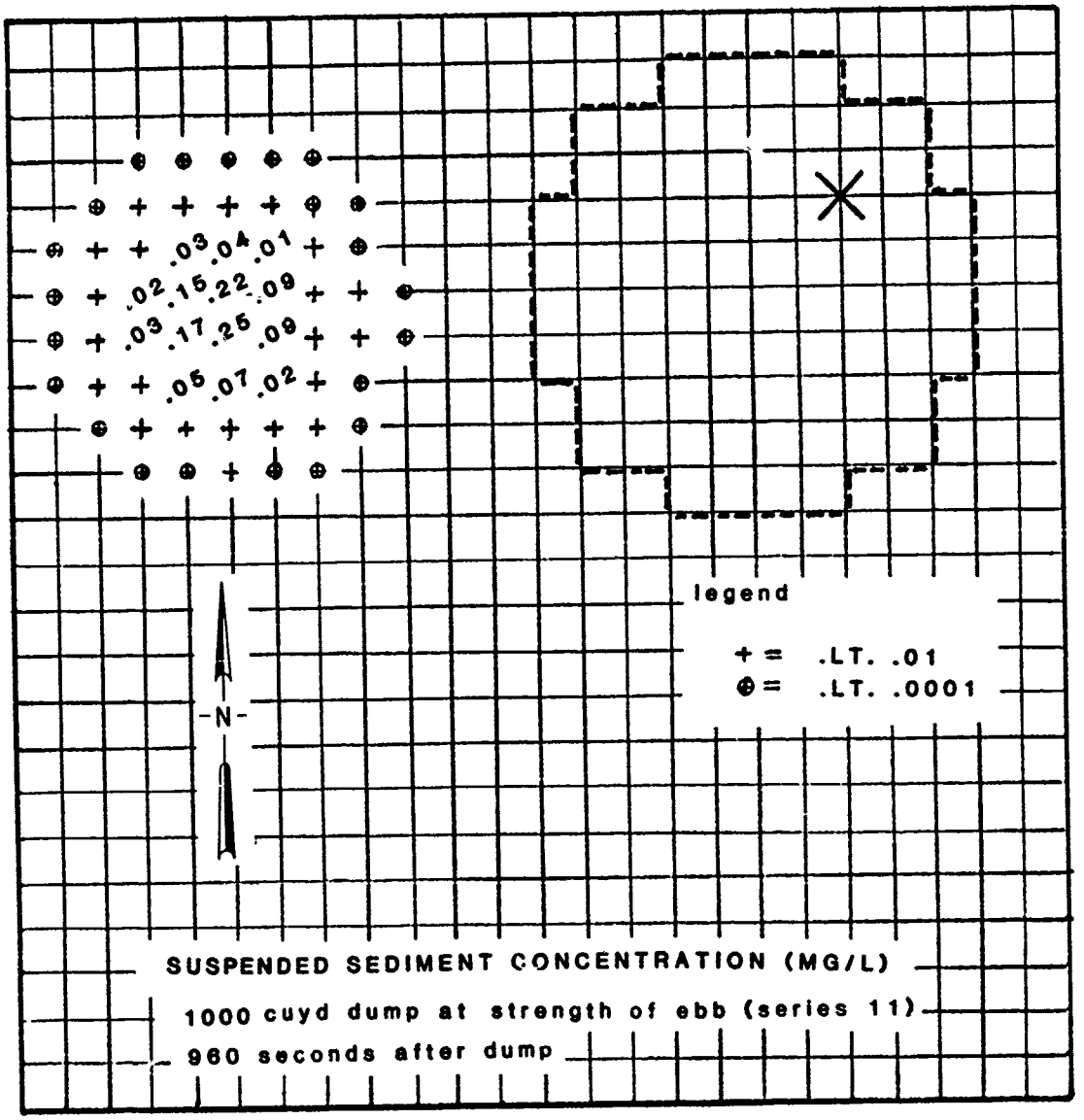

Figure A9. Suspended sediment concentration from dump of dredged material with 30 percent of clay-silt fraction as clumps

APPENDIX B: ACKERS-WHITE SAND-TRANSPORT CALCULATIONS

Dimensionless grain diameter D_{gr}

$$D_{gr} = D\left[\frac{g(s-1)}{\nu^2}\right]^{1/3}$$

where

D = representative grain diameter = 0.0002 m

g = acceleration due to gravity = 9.81 m/sec^2

s = mass density of sediment relative to that of fluid = 2.60

ν = kinematic viscosity of fluid = 1×10^{-6} m^2/sec

$$D_{gr} = 4.96$$

Sediment mobility F_{gr}

$$F_{gr} = \frac{v_*^n}{\sqrt{gD(s-1)}}\left(\frac{V}{\sqrt{32}\log\frac{\alpha d}{D}}\right)^{1-n}$$

where

v_* = shear velocity from Manning's shear stress equation
= $(\sqrt{gNV})/d^{1/6}$

N = Manning's friction factor = 0.015

V = tidal current, m/sec

d = mean depth of flow = 12.19 m

n = transition exponent based on sediment size = 1.0 ~ 0.56 log (D_{gr})
= 0.61

α = coefficient in rough-turbulent equation = 12.3

$$F_{gr} = 0.0022V$$

General transport function G_{gr}

$$G_{gr} = C\left(\frac{F_{gr}}{A} - 1\right)^{m}$$

where

C = coefficient for sediment transport function = 0.00943

A = value of F_{gr} at nominal initial motion = 0.243

m = exponent in sediment transport function = 3.29

$$G_{gr} = 0.00943\left(\frac{F_{gr}}{0.243} - 1\right)^{m}$$

Sediment flux (X)

$$X = \frac{G_{gr}\, sDV^{n}}{d\nu_{*}^{n}} \text{ (mass flux per unit mass flow rate)}$$

$$X = 0.00138G_{gr}$$

Unit width mass flow rate (q)

$$q = \gamma_{w}Vd$$

where

q = 12,190V , kg/sec/m

γ_{w} = unit weight of water (γ_{w} = 1,000 kg/m^3)

Unit width sand transport by weight (T)

T = Xq

T = $(0.00138G_{gr})$ (12,190V), kg/sec/m

T = $16.82G_{gr}V$, kg/sec/m

Results

The curve relating the sand transport capability at the mound (in lb/min/ft) to tidal current (in fps) is shown in Figure B1. As shown, tidal currents of about 3 fps are required for sand movement to begin. Tabulated results of sand movement over a tidal cycle for Series 11, 12, 21, 22, 31, and XX conditions are given in Tables B1-B6, respectively.

Table B1

Transport Potential for Sand Based on Ackers-White Method

Series 11

ATU	Velocity, fps	Transport, T , lb/min/ft
0	3.4	3
1	2.7	0
2	1.4	0
3	0.7	0
4	1.8	0
5	2.4	0
6	2.9	0
7	3.2	2
8	3.4	3
9	3.3	3
10	2.8	0
11	2.1	0
12	1.1	0
13	1.5	0
14	2.8	0
15	4.6	30
16	5.5	60
17	6.1	135
18	6.3	165
19	6.0	130
20	5.5	80
21	4.9	40
22	4.1	15
23	2.5	0
24	0.5	0
25	1.6	0
26	2.3	0
27	3.2	2
28	3.5	6
29	3.7	9
30	3.6	8
31	3.5	6
32	2.9	0
33	1.5	0
34	0.3	0
35	1.9	0
36	3.2	2
37	4.0	13
38	4.4	25
39	4.1	15
TOTAL		28,200 lb/tidal cycle/ft

Note: ATU = Acquisition Time Unit (1 ATU = 37.5 min).

Table B2

Transport Potential for Sand Based on Ackers-White Method

Series 12

ATU	Velocity, fps	Transport, T , lb/min/ft
0	3.5	6
1	3.0	1
2	2.1	0
3	0.5	0
4	1.3	0
5	2.4	0
6	3.1	1
7	3.6	8
8	3.9	12
9	3.8	10
10	3.4	3
11	2.5	0
12	0.9	0
13	1.7	0
14	3.5	6
15	4.6	30
16	5.3	65
17	6.1	135
18	6.2	150
19	6.3	165
20	6.1	135
21	5.2	150
22	4.0	55
23	2.9	13
24	0.7	0
25	1.5	0
26	2.7	0
27	3.2	2
28	3.7	9
29	4.3	20
30	4.4	25
31	3.7	9
32	3.0	1
33	2.0	0
34	0.6	0
35	1.8	0
36	3.2	2
37	3.7	9
38	4.1	15
39	3.6	9
TOTAL		33,600 lb/tidal cycle/ft

Note: ATU = Acquisition Time Unit (1 ATU = 37.5 min).

Table B3

Transport Potential for Sand Based on Ackers-White Method

Series 21

ATU	Velocity, fps	Transport, T , lb/min/ft
0	1.2	0
1	0.5	0
2	2.3	0
3	4.7	32
4	5.5	60
5	6.0	130
6	6.0	130
7	5.7	95
8	5.2	55
9	4.4	25
10	2.8	0
11	0.6	0
12	1.8	0
13	2.7	0
14	3.5	6
15	4.2	18
16	4.2	18
17	4.1	15
18	3.5	6
19	2.6	0
20	1.1	0
21	1.5	0
22	3.7	9
23	4.6	30
24	5.8	105
25	6.3	165
26	6.5	190
27	6.3	165
28	5.5	60
29	4.0	13
30	2.2	0
31	1.0	0
32	1.9	0
33	2.7	0
34	3.5	6
35	4.0	13
36	4.2	18
37	4.0	13
38	3.3	3
39	2.2	0
TOTAL		51,800 lb/tidal cycle/ft

Note: ATU = Acquisition Time Unit (1 ATU = 37.5 min).

Table B4

Transport Potential for Sand Based on Ackers-White Method

Series 22

ATU	Velocity, fps	Transport, T , lb/min/ft
0	0.5	0
1	2.2	0
2	4.1	15
3	4.9	40
4	5.3	65
5	5.9	115
6	5.8	105
7	5.7	95
8	5.5	80
9	4.7	32
10	3.2	2
11	0.7	0
12	1.6	0
13	2.9	0
14	3.9	12
15	4.7	32
16	4.5	25
17	3.9	12
18	3.4	3
19	3.0	1
20	1.4	0
21	1.0	0
22	3.3	3
23	5.1	50
24	5.6	90
25	6.1	135
26	6.2	150
27	6.2	150
28	5.7	95
29	4.5	25
30	2.8	0
31	0.5	0
32	2.0	0
33	2.8	0
34	3.6	9
35	4.4	25
36	4.3	20
37	3.9	12
38	3.3	3
39	2.2	0
TOTAL		46,900 lb/tidal cycle/ft

Ncte: ATU = Acquisition Time Unit (1 ATU = 37.5 min).

Table B5

Transport Potential for Sand Based on Ackers-White Method

Series 31

ATU	Velocity, fps	Transport, T , lb/min/ft
0	3.4	3
1	2.9	0
2	1.6	0
3	0.2	0
4	1.3	0
5	2.0	0
6	2.5	0
7	3.0	1
8	3.4	3
9	2.2	0
10	2.8	0
11	2.0	0
12	0.2	0
13	2.7	0
14	4.1	15
15	5.4	70
16	6.4	175
17	6.9	260
18	7.5	400
19	7.5	400
20	7.2	325
21	6.6	205
22	5.4	70
23	4.2	18
24	2.2	0
25	0.5	0
26	1.8	0
27	2.7	0
28	3.6	8
29	4.1	15
30	3.8	10
31	3.7	9
32	3.4	3
33	2.7	0
34	2.2	0
35	1.0	0
36	0.5	0
37	1.6	0
38	3.5	6
39	3.4	3
TOTAL		75,000 lb/tidal cycle/ft

Note: ATU = Acquisition Time Unit (1 ATU = 37.5 min).

Table B6

Transport Potential for Sand Based on Ackers-White Method

Series XX

ATU	Velocity, fps	Transport, T , lb/min/ft
0	2.3	0
1	1.8	0
2	0.9	0
3	0.5	0
4	1.2	0
5	1.6	0
6	1.9	0
7	2.1	0
8	2.3	0
9	2.2	0
10	1.9	0
11	1.4	0
12	0.7	0
13	1.0	0
14	1.9	0
15	3.1	1
16	3.7	9
17	4.1	15
18	4.2	18
19	4.0	13
20	3.7	9
21	3.3	3
22	2.7	0
23	1.7	0
24	0.3	0
25	1.1	0
26	1.5	0
27	2.1	0
28	2.3	0
29	2.5	0
30	2.4	0
31	2.3	0
32	1.9	0
33	1.0	0
34	0.2	0
35	1.3	0
36	2.1	0
37	2.7	0
38	2.9	0
39	2.7	0
TOTAL		2,600 lb/tidal cycle/ft

Note: ATU = Acquisition Time Unit (1 ATU = 37.5 min).

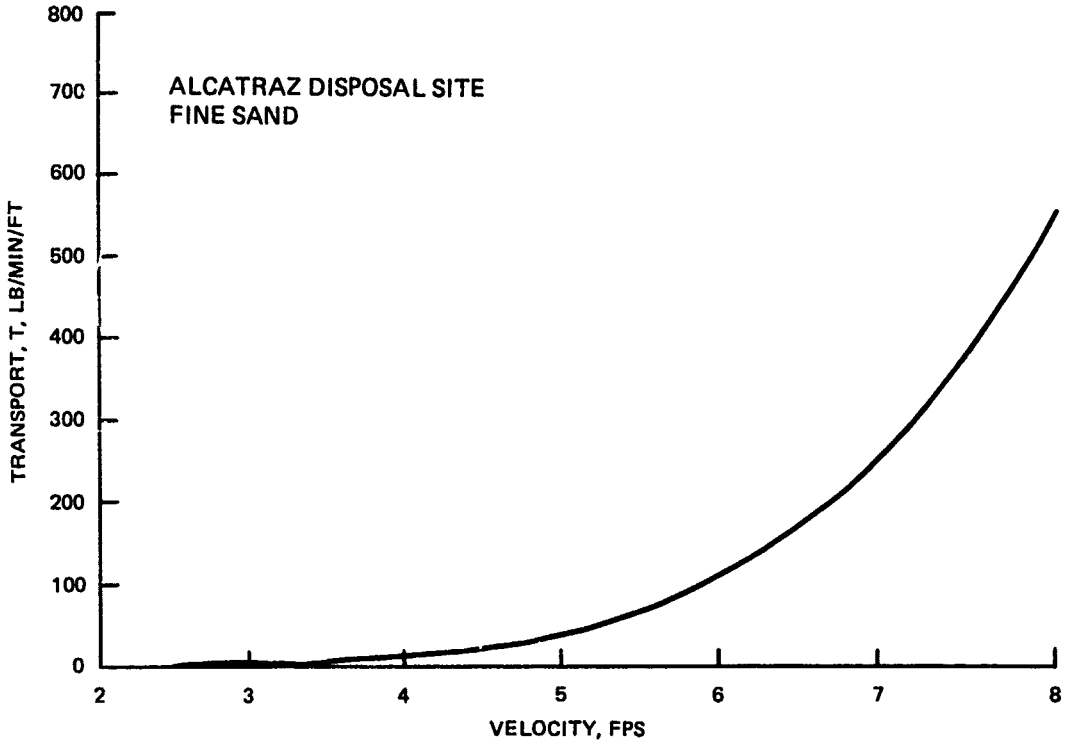

Figure B1. Transport potential of sand at mound as a function of current speed based on Ackers-White method

APPENDIX C: MODIFIED PARTHENAIDES CLAY-SILT RESUSPENSION CALCULATIONS

Erosion rate (S)

$$S = M\left(\frac{\tau_B}{\tau_e} - 1\right) \text{ (kg/sec/m)}$$

where

M = erosion rate constant, kg/sec/m^2

= 0.002 kg/sec/m^2 for unconsolidated material

= 0.0005 kg/sec/m^2 for clumps

τ_B = Bed shear stress, N/m^2

= $(\rho g n^2 V^2 / d^{1/3})$

ρ = 1,000 kg/m^3 (fluid density)

g = 9.81 m/sec^2 (acceleration due to gravity)

n = 0.015 (Manning's friction factor)

V = tidal current, m/sec

d = 12.19 m (water depth)

τ_e = critical shear stress for erosion, N/m^2

= 0.10 N/m^2 for unconsolidated material

= 1.0 N/m^2 for clumps

Therefore

$Su = 0.0194V^2 - 0.002$, kg/sec/m^2 (unconsolidated)

$Sc = 0.000485V^2 - 0.0005$, kg/sec/m^2 (clumps)

Results

The curves relating clay-silt resuspension capability at the mound (in lb/min/sq ft) to tidal current (in fps) are shown in Figure C1. Tabulated results of clay-silt resuspension summed over a tidal cycle (in lb/sq ft) for Series 11, 12, 21, 22, 31, and XX are given in Tables C1-C6, respectively.

Table C1

Resuspension Potential for Clay-Silt Based on Modified Parthenaides Equation, Series 11

ATU	Velocity, fps	Su , lb/sq ft/min	Sc , lb/sq ft/min
0	3.4	0.23	0.00
1	2.7	0.13	0.00
2	1.4	0.02	0.00
3	0.7	0.00	0.00
4	1.8	0.05	0.00
5	2.4	0.10	0.00
6	2.9	0.16	0.00
7	3.2	0.20	0.00
8	3.4	0.23	0.00
9	3.3	0.22	0.00
10	2.8	0.15	0.00
11	2.1	0.07	0.00
12	1.1	0.01	0.00
13	1.5	0.02	0.00
14	2.8	0.15	0.00
15	4.6	0.44	0.01
16	5.5	0.64	0.01
17	.1	0.80	0.01
18	6.3	0.84	0.02
19	6.0	0.76	0.01
20	5.5	0.64	0.01
21	4.9	0.50	0.01
22	4.1	0.35	0.00
23	2.5	0.11	0.00
24	0.5	0.00	0.00
25	1.6	0.03	0.00
26	2.3	0.09	0.00
27	3.2	0.20	0.00
28	3.5	0.24	0.00
29	3.7	0.27	0.00
30	3.6	0.26	0.00
31	3.5	0.25	0.00
32	2.9	0.16	0.00
33	1.5	0.02	0.00
34	0.3	0.00	0.00
35	1.9	0.05	0.00
36	3.2	0.20	0.00
37	4.0	0.33	0.00
38	4.4	0.41	0.01
39	4.1	0.35	0.00
TOTAL		363 lb/sq ft/ tidal cycle	3.4 lb/sq ft/ tidal cycle

Note: ATU = Acquisition Time Unit (1 ATU = 37.5 min).

Table C2

Resuspension Potential for Clay-Silt Based on Modified Parthenaides Equation, Series 12

ATU	Velocity, fps	Su , lb/sq ft/min	Sc , lb/sq ft/min
0	3.5	0.24	0.00
1	3.0	0.17	0.00
2	2.1	0.07	0.00
3	0.5	0.00	0.00
4	1.3	0.01	0.00
5	2.4	0.10	0.00
6	3.1	0.18	0.00
7	3.6	0.26	0.00
8	3.9	0.31	0.00
9	3.8	0.29	0.00
10	3.4	0.23	0.00
11	2.5	0.11	0.00
12	0.9	0.00	0.00
13	1.7	0.04	0.00
14	3.5	0.24	0.00
15	4.6	0.44	0.01
16	5.3	0.59	0.01
17	6.1	0.80	0.01
18	6.2	0.82	0.02
19	6.3	0.84	0.02
20	6.1	0.80	0.01
21	5.2	0.57	0.01
22	4.0	0.33	0.00
23	2.9	0.16	0.00
24	0.7	0.00	0.00
25	1.5	0.02	0.00
26	2.7	0.13	0.00
27	3.2	0.20	0.00
28	3.7	0.27	0.00
29	4.3	0.38	0.01
30	4.4	0.41	0.01
31	3.7	0.27	0.00
32	3.0	0.17	0.00
33	2.0	0.06	0.00
34	0.6	0.00	0.00
35	1.8	0.05	0.00
36	3.2	0.20	0.00
37	3.7	0.27	0.00
38	4.1	0.35	0.00
39	3.6	0.26	0.00
TOTAL		390 lb/sq ft/ tidal cycle	4.2 lb/sq ft/ tidal cycle

Note: ATU = Acquisition Time Unit (1 ATU = 37.5 min).

Table C3

Resuspension Potential for Clay-Silt Based on Modified Parthenaides Equation, Series 21

ATU	Velocity, fps	Su , lb/sq ft/min	Sc , lb/sq ft/min
0	1.2	0.01	0.00
1	0.5	0.00	0.00
2	2.3	0.09	0.00
3	4.7	0.46	0.01
4	5.5	0.64	0.01
5	6.0	0.76	0.01
6	6.0	0.76	0.01
7	5.7	0.68	0.01
8	5.2	0.57	0.01
9	4.4	0.40	0.01
10	2.8	0.15	0.00
11	0.6	0.00	0.00
12	1.8	0.05	0.00
13	2.7	0.13	0.00
14	3.5	0.24	0.00
15	4.2	0.37	0.01
16	4.2	0.37	0.01
17	4.1	0.35	0.00
18	3.5	0.24	0.00
19	2.6	0.12	0.00
20	1.1	0.00	0.00
21	1.5	0.02	0.00
22	3.7	0.27	0.00
23	4.6	0.44	0.01
24	5.8	0.71	0.01
25	6.3	0.85	0.02
26	6.5	0.92	0.02
27	6.3	0.85	0.02
28	5.5	0.64	0.01
29	4.0	0.33	0.00
30	2.2	0.08	0.00
31	1.0	0.00	0.00
32	1.9	0.05	0.00
33	2.7	0.13	0.00
34	3.5	0.24	0.00
35	4.0	0.33	0.00
36	4.2	0.37	0.01
37	4.0	0.33	0.00
38	3.3	0.21	0.00
39	2.2	0.08	0.00
TOTAL		497 lb/sq ft/ tidal cycle	7.2 lb/sq ft/ tidal cycle

Note: ATU = Acquisition Time Unit (1 ATU = 37.5 min).

Table C4

Resuspension Potential for Clay-Silt Based on Modified Parthenaides Equation, Series 22

ATU	Velocity, fps	Su , lb/sq ft/min	Sc , lb/sq ft/min
0	0.5	0.00	0.00
1	2.2	0.08	0.00
2	4.1	0.35	0.00
3	4.9	0.50	0.01
4	5.3	0.59	0.01
5	5.9	0.73	0.02
6	5.8	0.71	0.01
7	5.7	0.68	0.01
8	5.5	0.64	0.01
9	4.7	0.46	0.01
10	3.2	0.20	0.00
11	0.7	0.00	0.00
12	1.6	0.03	0.00
13	2.9	0.16	0.00
14	3.9	0.31	0.00
15	4.7	0.46	0.01
16	4.5	0.42	0.01
17	3.9	0.31	0.00
18	3.4	0.23	0.00
19	3.0	0.17	0.00
20	1.4	0.02	0.00
21	1.0	0.00	0.00
22	3.3	0.22	0.00
23	5.1	0.54	0.01
24	5.6	0.66	0.01
25	6.1	0.80	0.02
26	6.2	0.82	0.02
27	6.2	0.82	0.02
28	5.7	0.68	0.01
29	4.5	0.42	0.01
30	2.8	0.15	0.00
31	0.5	0.00	0.00
32	2.0	0.06	0.00
33	2.8	0.15	0.00
34	3.6	0.26	0.00
35	4.4	0.41	0.01
36	4.3	0.38	0.01
37	3.9	0.31	0.00
38	3.3	0.21	0.00
39	2.2	0.08	0.00
TOTAL		508 lb/sq ft/ tidal cycle	8.0 lb/sq ft/ tidal cycle

Note: ATU = Acquisition Time Unit (1 ATU = 37.5 min).

Table C5

Resuspension Potential for Clay-Silt Based on Modified Parthenaides Equation, Series 31

ATU	Velocity, fps	Su , lb/sq ft/min	Sc , lb/sq ft/min
0	3.4	0.23	0.00
1	2.9	0.16	0.00
2	1.6	0.03	0.00
3	0.2	0.00	0.00
4	1.3	0.01	0.00
5	2.0	0.06	0.00
6	2.5	0.11	0.00
7	3.0	0.17	0.00
8	3.4	0.23	0.00
9	3.2	0.20	0.00
10	2.8	0.15	0.00
11	2.0	0.06	0.00
12	0.2	0.00	0.00
13	2.7	0.13	0.00
14	4.1	0.35	0.00
15	5.4	0.62	0.01
16	6.4	0.88	0.02
17	6.9	1.02	0.02
18	7.5	1.23	0.03
19	7.5	1.23	0.03
20	7.2	1.13	0.03
21	6.6	0.94	0.02
22	5.4	0.62	0.01
23	4.2	0.37	0.01
24	2.2	0.08	0.00
25	0.5	0.00	0.00
26	1.8	0.05	0.00
27	2.7	0.13	0.00
28	3.6	0.26	0.00
29	4.1	0.35	0.00
30	3.8	0.29	0.00
31	3.7	0.27	0.00
32	3.4	0.23	0.00
33	2.7	0.13	0.00
34	2.2	0.08	0.00
35	1.0	0.00	0.00
36	0.5	0.00	0.00
37	1.6	0.03	0.00
38	3.5	0.25	0.00
39	3.4	0.23	0.00
TOTAL		462 lb/sq ft/ tidal cycle	6.8 lb/sq ft/ tidal cycle

Note: ATU = Acquisition Time Unit (1 ATU = 37.5 min).1

Table C6

Resuspension Potential for Clay-Silt Based on Modified Parthenaides Equation, Series XX

ATU	Velocity, fps	Su , lb/sq ft/min	Sc , lb/sq ft/min
0	2.3	0.09	0.00
1	1.8	0.05	0.00
2	0.9	0.00	0.00
3	0.5	0.00	0.00
4	1.2	0.01	0.00
5	1.6	0.03	0.00
6	1.9	0.05	0.00
7	2.1	0.07	0.00
8	2.3	0.09	0.00
9	2.2	0.08	0.00
10	1.9	0.05	0.00
11	1.4	0.02	0.00
12	0.7	0.00	0.00
13	1.0	0.00	0.00
14	1.9	0.05	0.00
15	3.1	0.18	0.00
16	3.7	0.27	0.00
17	4.1	0.35	0.00
18	4.2	0.37	0.01
19	4.0	0.33	0.00
20	3.7	0.33	0.00
21	3.3	0.22	0.00
22	2.7	0.13	0.00
23	1.7	0.04	0.00
24	0.3	0.00	0.00
25	1.1	0.01	0.00
26	1.5	0.02	0.00
27	2.1	0.07	0.00
28	2.3	0.09	0.00
29	2.5	0.11	0.00
30	2.4	0.10	0.00
31	2.3	0.09	0.00
32	1.9	0.05	0.00
33	1.0	0.00	0.00
34	0.2	0.00	0.00
35	1.3	0.01	0.00
36	2.1	0.07	0.00
37	2.7	0.13	0.00
38	2.9	0.16	0.00
39	2.7	0.13	0.00
TOTAL		140 lb/sq ft/ tidal cycle	0.4 lb/sq ft/ tidal cycle

Note: ATU = Acquisition Time Unit (1 ATU = 37.5 min).

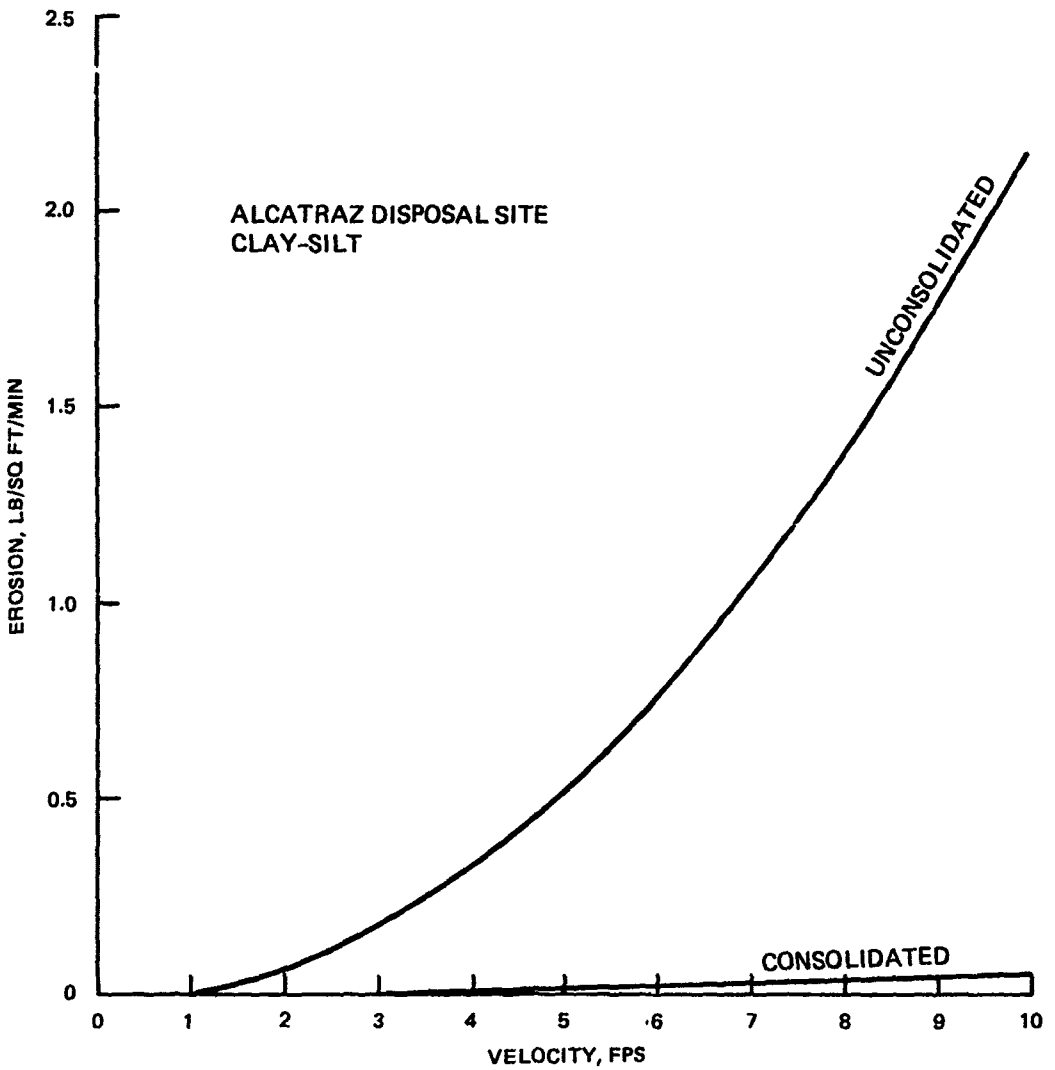

Figure C1. Erosion potential of clay-silt at mound (both consolidated and unconsolidated) as a function of current speed based on modified Parthenaides equation